设计指南：TIDEP-01012
采用级联毫米波传感器的成像雷达参考设计

说明

此参考设计为级联成像雷达射频系统奠定了基础。级联雷达器件可支持远距离雷达 (LRR) 波束形成 应用 以及具有增强的角分辨率性能的中距离 (MRR) 和短距离雷达 (SRR) MIMO 应用 。

AWR2243 级联雷达射频开发套件用于通过多器件、波束形成配置估算和跟踪物体在 350 米以外的位置（在方位平面中）。另外，该系统在 TDMA-MIMO 配置中具有低至 1.4 度的方位角分辨率。

此设计指南中提供的数据是从使用 AWR1243P 器件的 MMWCAS-RF-EVM 版本 C 获得的。然而，最新的 MMWCAS-RF-EVM 版本 D 使用了第二代 AWR2243 器件。此 AWR2243 解决方案应该作为未来设计的参考。

资源

TIDEP-01012	设计文件夹
AWR2243	产品文件夹
LP87524P-Q1	产品文件夹
TMP112	产品文件夹
MMWCAS-RF-EVM	工具文件夹

Search Our E2E™ support forums

特性

- 适用于 LRR、MRR 和 SRR 应用的双芯片或四芯片 FMCW 雷达
- 借助 35cm 的距离分辨率检测 350m 以外的物体（例如，汽车和卡车）；人类 RCS 物体的可检测距离为 150m
- 天线视场为 ±70º，且角分辨率约为 1.4 度
- 提供 MATLAB MIMO 和波束形成示例代码
- 基于 AWR2243 的演示设计
- 全面说明了级联成像雷达前端波束形成和 MIMO 配置

应用

- 远距离雷达
- 成像雷达
- 交通监控摄像头

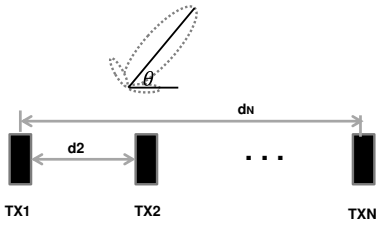

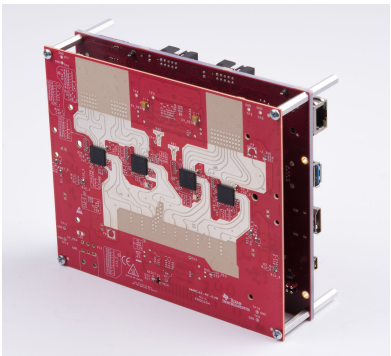

1 System Description

ADAS control of a vehicle provides quality-of-life and safety benefits in addition to making the relatively mundane act of driving safer and less difficult. The quality-of-life features include the ability of a vehicle to park itself, or to determine whether a lane change is possible, and provide features like automatic cruise control—where a vehicle maintains a constant distance with respect to the car ahead of it, essentially, tracking the velocity of the car in front of it. Autonomous braking and collision avoidance are safety features that prevent accidents caused by driver inattention. These features work by observing the area in front of a car and alerting the ADAS subsystems if obstacles are observed that are likely to hit the car. Implementing these technologies requires a variety of sensors to detect obstacles in the environment and track their velocities and positions over time.

1.1 Why Cascade Radar?

Frequency-modulated continuous-wave (FMCW) radars allow the accurate measurement of range and relative velocity of obstacles and other vehicles; therefore, radars are useful for autonomous vehicular applications (such as parking assist and lane change assist) and car safety applications (autonomous breaking and collision avoidance). An important advantage of radars over camera and light-detection-and-ranging (LIDAR)-based systems is that radars are relatively immune to environmental conditions (such as the effects of rain, dust, and smoke). FMCW radars can work in complete darkness and also bright daylight (radars are not affected by glare) because they transmit and receive electromagnetic waves. When compared with ultrasound, radars typically have a much longer range and much faster time of transit for their signals.

Despite the many advantages of radar technology, in many cases, automotive manufacturers today still use camera sensors as the primary sensor technology used to make final safety decisions in the system.

The radar sensor is being used as the secondary sensor; meaning, the vehicle system receives the Radar warning, but decides to take an action only upon the camera sensor verification. The main reason is limitation in radar angular resolution. The radar sensors deployed today in most vehicles lack the ability to distinguish between static objects with the same range and same relative velocity.

Today, a typical front radar sensor has about a 5-degree angular resolution that corresponds to the ability of the sensor to distinguish between objects that are 8.5 m apart at 100 m. Objects that are closer than 8.5 m appear as one object. For example, a vehicle stopped in the right lane, might look like a shoulder road street lamp for example, and therefore would be ignored by the safety system.

This is about to change with the introduction of the Imaging Radar solution from Texas Instruments (TI).

The TI Imaging Radar is a four-chip cascade solution, that acts like a single-chip sensor but achieves $20Log10(N_{TX})$ SNR gain in TX beamforming mode and 360/(N*pi) angular resolution (N is the number of virtual antennas in a MIMO configuration).

Using the TI Imaging Radar solution, we can distinguish between static objects 0.6 degrees apart with all antennae placed in single dimension linearly, and reach a 350-m object detecting range(angular resolution is dependent on the antenna configuration and the number of TX/RX antennae).

This performance enables TI Imaging Radar to become the primary sensor in the vehicle and enhance safety across weather and visibility conditions by providing a high-resolution image for both static and moving objects.

1.2 TI Cascade Radar Design

TIDEP-01012 is an introductory application that demonstrates both a long-range beam-forming configuration, and a shorter range, high-angular resolution MIMO configuration. This reference design can be used as a starting point to design a standalone sensor for a variety of long range and imaging radar applications. The TI Cascade RF reference design has demonstrated automobile target detection in excess of 350 m along with 1.4 degree angular resolution.

The flexible chirp and frame timing engine available on the AWR2243 device (similar to other AWR family mmWave sensors) allows the system to function as a multi-mode radar, interleaving beam-forming and MIMO configurations on a per frame basis. This enables the sensor designer to achieve best range and best angular resolution across the array of Cascaded AWR2243 devices as the scene dynamics requires.

Beamforming antenna across multiple, cascaded, AWR2243 devices provide sensor designers with higher-output power and therefore lower-detectable target RCS, or increased range detection, or both. Applications requiring detection of automobile, motorcycle, pedestrian, signage, bridges, and other roadway objects and barriers at or beyond 350-m range can use this mode of operation.

In medium-range applications (150 m ranges), creating MIMO antenna arrays across multiple, cascaded, AWR2243 devices allows the sensor designer to maximize the number of active antenna enabling substantially improved angular resolution. This enables sub 1 degree resolution: true imaging radar capability.

图 1. AWR2243 Four-Device Cascade Radar RF Radar Board

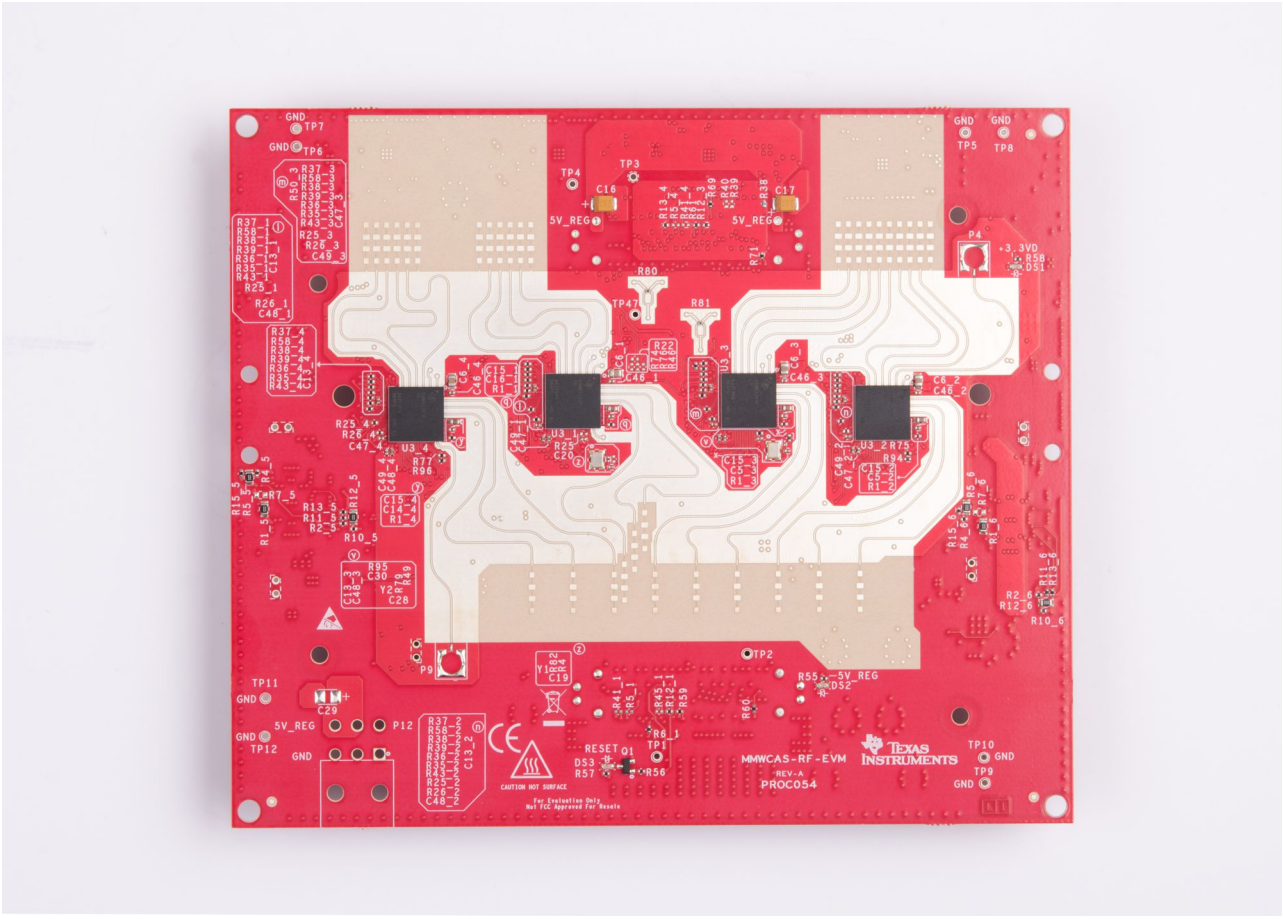

1.3 Key System Specifications

This reference design has two sets of specifications because the radar is used as a multi-mode radar. MIMO is the first specification. TX beamforming (TXBF) is the second specification,

表 **1. Key System Specifications**

PARAMETERS	SPECIFICATIONS (MIMO)	SPECIFICATIONS (TXBF)	DESCRIPTION
Maximum Range	150 m	350 m	This represents the maximum distance that the radar can detect an object representing an RCS of approximately 10 m^2
Range Resolution	60 cm	150 cm	Range resolution is the ability of a radar system to distinguish between two or more targets on the same bearing but at different ranges. The resolution is configurable, so the provided number is just an example.
Azimuth Angle Resolution	1.4 degrees	1.4 degrees (with multiple beam steering)	Angle resolution is the ability of a radar system to distinguish between two or more targets with the same range and velocity but different angles. The resolution is equivalent in both applications.
Elevation Angle Resolution	18 degrees	n/a	Elevation angle resolution is only available for MIMO application given the antenna design on the TI cascade EVM board.
Maximum Velocity	133 kmph	133 kmph	This is the native maximum velocity obtained using a two-dimensional FFT on the frame data. For TDM MIMO case, velocity compensation algorithm is applied to recover the native maximum velocity. This specification will be improved over time by showing how higher-level algorithms can extend the maximum measurable velocity beyond this limit.
Velocity Resolution	0.53 kmph	0.53 kmph	This parameter represents the capability of the radar sensor to distinguish between two or more objects at the same range but moving with different velocities.

2 System Overview

2.1 Block Diagram

图 2 shows the block diagram of the cascade RF board.

图 2. Cascade Radar RF Board System Block Diagram

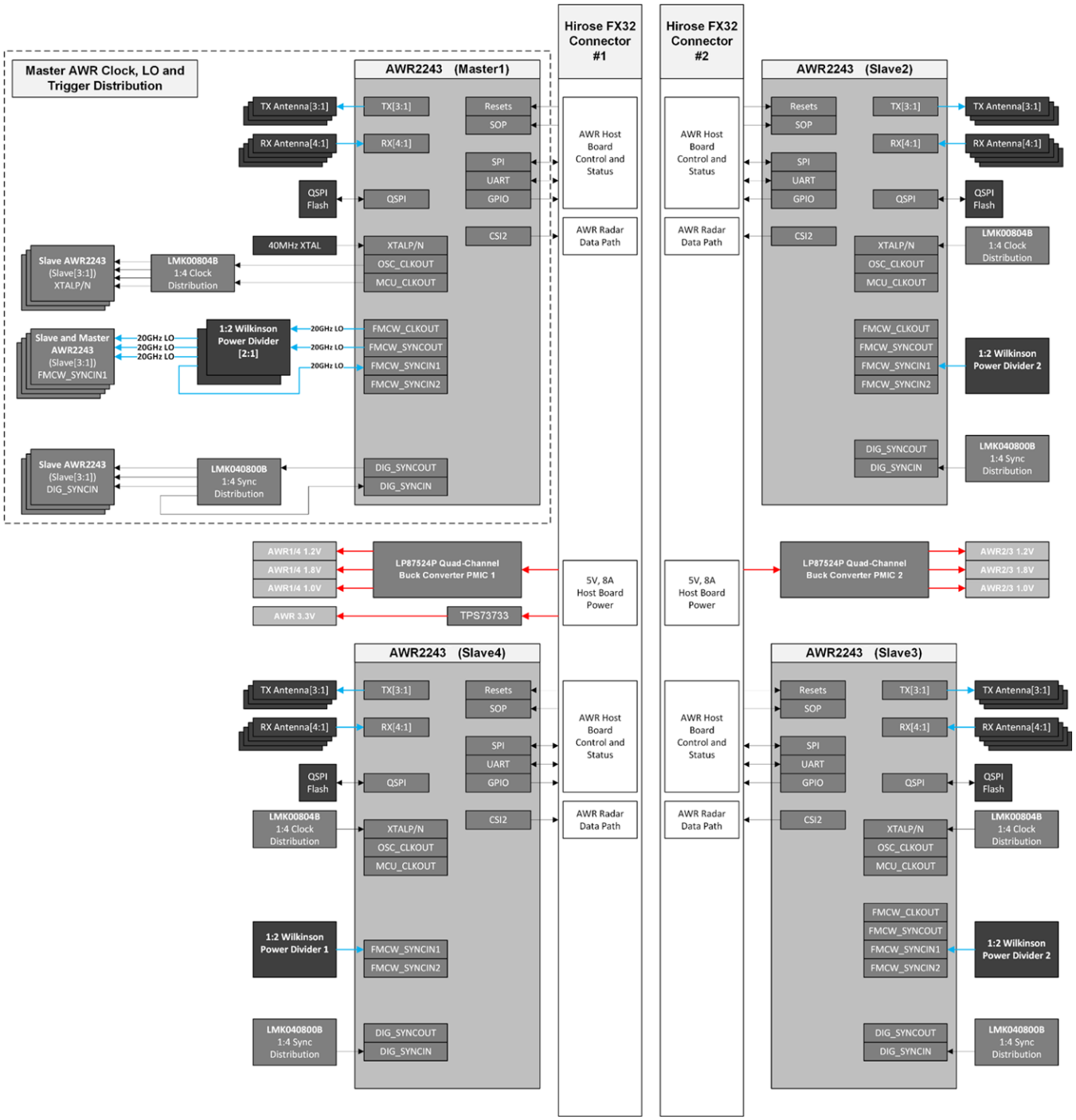

2.2 Highlighted Products

The AWR2243 is an integrated single-chip, frequency modulated continuous wave (FMCW) sensor capable of operation in the 76 to 81 GHz frequency band. The device is built with TI's low-power, 45-nm RFCMOS processor and enables unprecedented levels of analog and digital integration in an extremely small form factor. The device has four receivers and three transmitters with a closed-loop phase-locked loop (PLL) for precise and linear chirp synthesis.

Each transmitter includes a programmable 6-bit phase shifter (5.625 degree step) to enable beam-forming applications. Each devices also includes two 20-GHz local oscillator (LO) output and two 20-GHz LO input paths for sharing the VCO output with neighboring devices. This enables a cost-effective, totally passive, cascaded radar architecture.

The sensor includes a built-in radio processor (BIST) for RF calibration and safety monitoring. Based on complex baseband architecture, the sensor device supports an IF bandwidth of 15 MHz with reconfigurable output sampling rates in both complex and real sampling modes. Two separate Arm® Cortex®-R4F based processors run the TI provided radar front-end, calibration, and host processor interface firmware targeting ASIL-B.

2.3 Design Considerations

2.3.1 AWR2243 Cascade RF Board Features

	Cascade Radar RF Board
4 × AWR2243 76-81GHz Radar SoC	Integrated VCO, LO distribution, PA, LNA, ADC, 3 TX and 4 RX Arm MCU R4 Controller
AWR RF Peripherals	
12 × TX, 16 × RX Antennas	12 total transmitters across all 4 AWR2243 devices16 total receivers across all 4 × AWR2243 devices
Azimuth Array	86 element virtual array – enabling 1.4 degree angular resolution
Elevation Array	4 element virtual array – enabling 18 degree angular resolution
Embedded Antenna	Rogers RO3003 4-element, series-fed, patch antenna
20 GHz LOStar Distribution	2 × passive Wilkinson Power dividers fed by the Master AWR2243 device LO output to Slave AWR2243 devices and Master AWR2243 device
AWR Digital Peripherals	
Clock Distribution	LMK00804B low-jitter clock distribution
Digital Sync Distribution	LMK00804B low-jitter clock distribution
CSI2.0 4-lane	600Mbps/Lane, max 2.4Gbps ADC IF data per device
QSPI Flash	16Mbit QSPI flash for AWR firmware updates
Serial Peripherals	SPI, I2C, UART, GPIO
System Temperature	TMP112 I2C Temperature Sensors
Power	
Radar Power Management IC (PMIC) Solution	2 × LP87524P-Q1 Quad-Channel, Integrated FET, Buck Converters and LC filtering solution

2.3.2 AWR2243 Cascade RF Board Architecture

The AWR2243 Cascade RF board consists of four AWR2243 77-GHz radar devices and their associated power, clocking, synchronization, LO, and RF circuits.

Each AWR2243 RF, RX, and TX port is routed to its own set of etched, patch antenna. Each AWR2243 on the RF board has a 4-port CSI2.0 transmitter that is used for sending radar data to a host processor CSI2.0 receiver set. The entire AWR2243 configuration, control, and reset lines are made available on two host-interface connectors implemented with Hirose FX32 series connectors.

The AWR2243 devices are separated into master and slave devices classes. AWR2243 #1, the master device, uses the AWR2243 architecture built in LO distribution, clock distribution and frame synchronization distribution to provide 40-MHz clock, 20-GHz LO and digital frame synchronization to other three slave devices – AWR2243 #2, #3 and #4. This allows the system to generate and receive coherent FMCW chirps across the 4 AWR2243 device array of transmitters and receivers; enabling beam-forming and MIMO operation across the array of devices.

The 20 GHz LO distribution follows the start-network configuration described in the AWR2243 Cascade Radar Application Note, SWRA574B. With the master AWR2243 #1 feeding a network of two Wilkinson power dividers, that provide synchronous LO for the Master and Slave RF PA and mixer subsystems. All clock distribution, synchronization distribution, and LO distribution requirements are documented in this referenced application note.

The Cascade RF board accepts 5V DC, 8 A (max) power through the host board connectors. The primary 5 V system rail can be converted into the various AWR2243 device rails by a pair of LP87524P, quad-channel, monolithic, buck-converters.

2.3.3 20 GHz Local Oscillator (LO) Distribution

20-GHz LO distribution to all AWR2243 devices is accomplished through an entirely passive, transmission-line and etched power divider network. By using the dual LO outputs and LO inputs provided on each AWR2243 device, all devices including the master device, receive the same master device generated LO output. This results in all package and die routing delays common across all devices. The PCB designer is left with the task of delay matching only the BGA to BGA delays.

By using both of the 6-dBm (typical) LO output, and minimizing transmission line and power divider losses, no external amplifiers are required to be added to the LO network. Additionally, by outputting 20 GHz LO versus full 77-GHz RF for RF synchronization, the LO PCB link budgets can be more relaxed.

The passive LO distribution network and relaxed link budget results in more PCB design flexibility and a lower overall system cost.

图 3 shows the block diagram of the delay matched LO distribution. 图 4 shows the implemented Wilkinson power dividers in GCPW transmission-line. Fanout from the AWR2243 devices and power dividers is through GCPW lines. The majority of the LO distribution length is carried through an internal Stripline layer.

图 3. 20 GHz LO Distribution Block Diagram

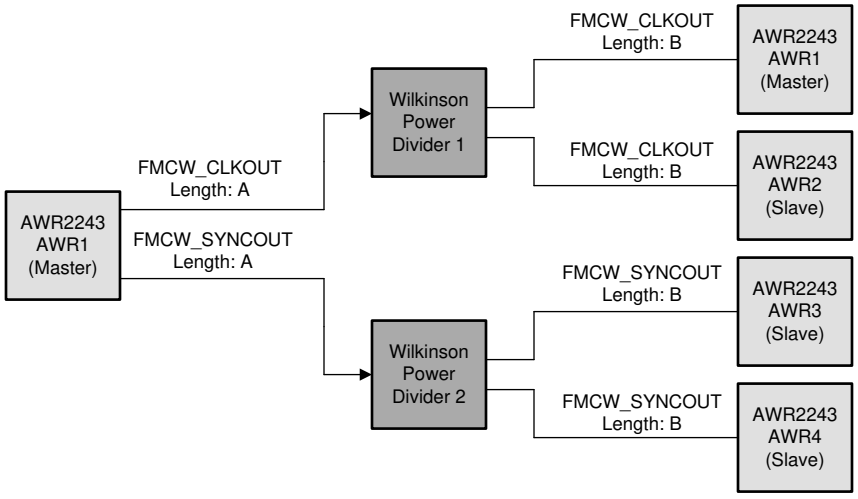

图 4. 20 GHz LO Distribution Board Implementation

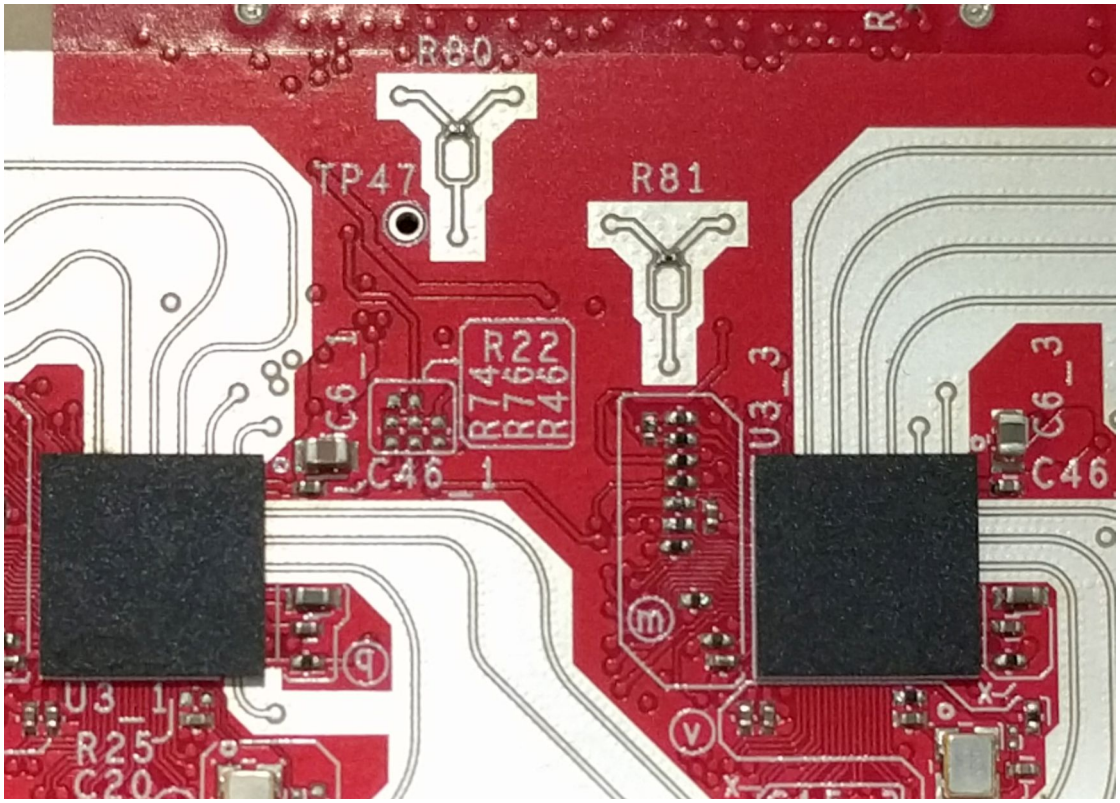

3 System Design Theory

The Cascade RF MIMO and beamforming antenna design, chirp, and frame configuration are system variables that must be co-designed for a particular application. Both the antenna array, MIMO chirp, and beamforming chirp design are presented here.

3.1 Antenna Configuration

图 5 shows the antenna array on the Cascade RF board with one master device and three slave devices. Together these devises create a total of 12 TX channels and 16 RX channels. Among the 12 TX channels, the three TXs (TX1/2/3) from the master device are placed in the vertical direction for elevation antenna estimation. The remaining 9 TXs (TX4 through TX12) and all 16 RX channels are placed in the horizontal plane for azimuth angle estimation. The relative distances between TXs and between RXs are shown in 图 6. The three elevation antennas are placed to form a minimum redundancy array to improve elevation angle resolution. Every two azimuth TXs are spaced 2 wavelengths apart. RX array A and RX array C are placed 16-wavelengths apart. RX array C and RX array B are placed four-wavelengths apart. The virtual array in MIMO mode is shown in 图 7, with 86 virtual antennas in azimuth direction. The overlapped antenna in azimuth is not shown in the figure. The elevation angle resolution is equivalent to the resolution achieved with 7 antennas.

图 5. Device and Antenna Array Groups

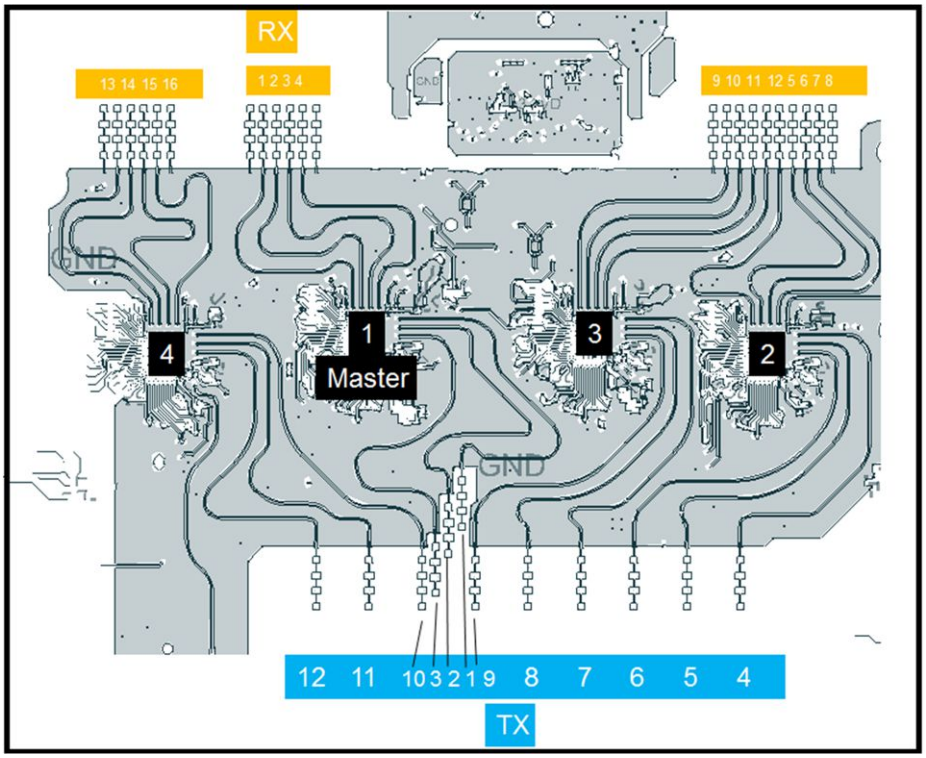

The Cascade RF board can also be used in two chip cascade mode with 6 TX and 8 RX channels highlighted in 图 6. 图 8 shows the virtual MIMO array in 2-device cascade mode using TX ID of [1 2 3 10 11 12] and RX ID of [4 3 2 1 16 15 14 13], with 23 azimuth antennas and same elevation configuration with 4-device cascade.

图 6. Antenna Array Positions

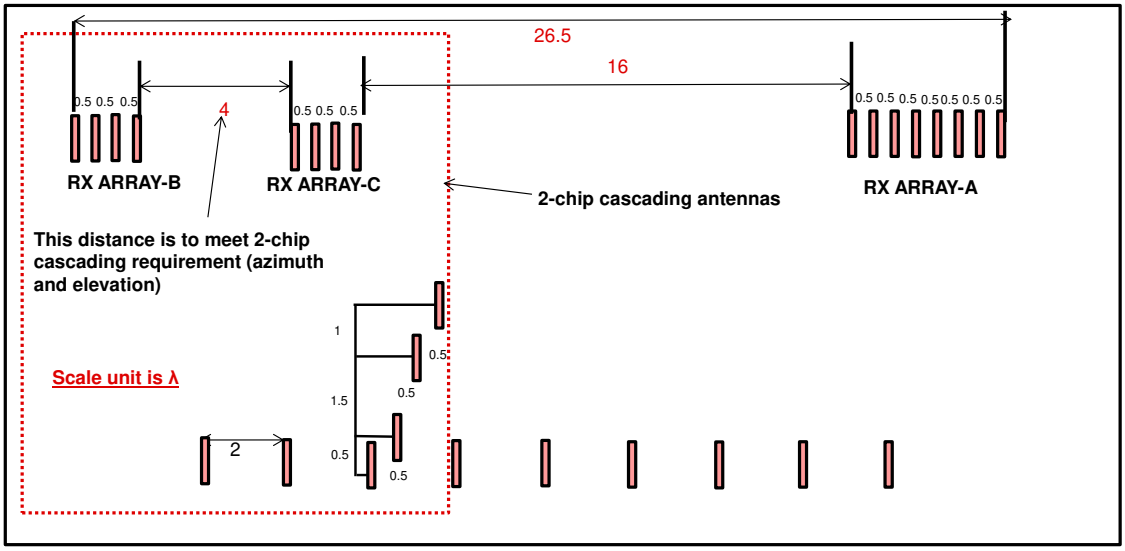

图 7. 4-Device Cascade Virtual MIMO Array with 12 TX and 16 RX

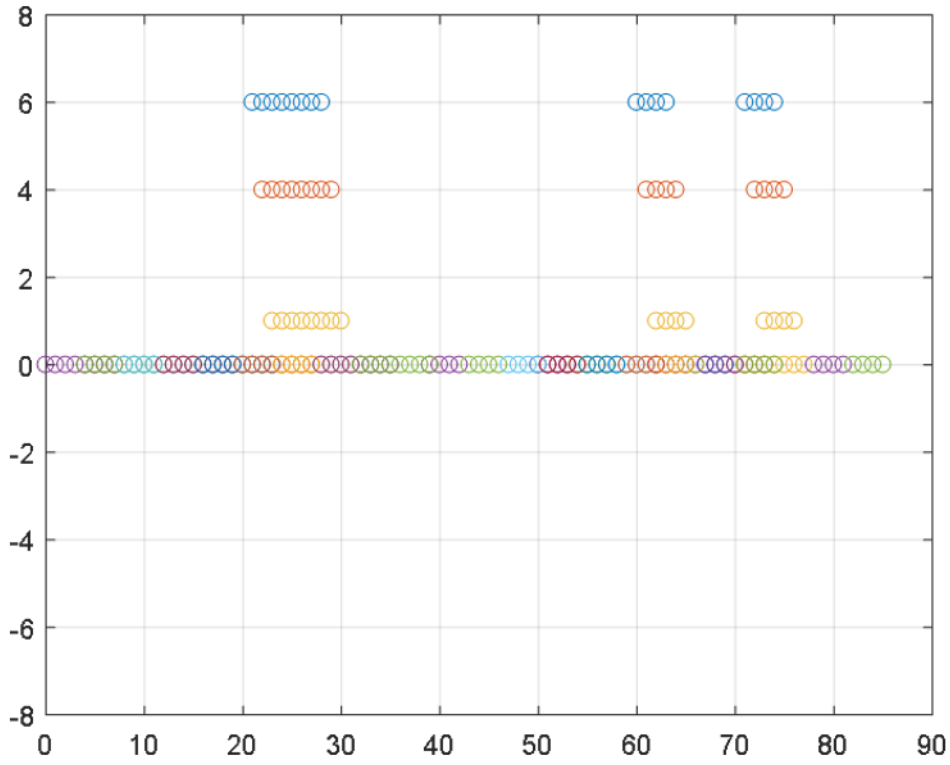

图 8. 2-Device Cascade Virtual MIMO Array with 6 TX and 8 RX

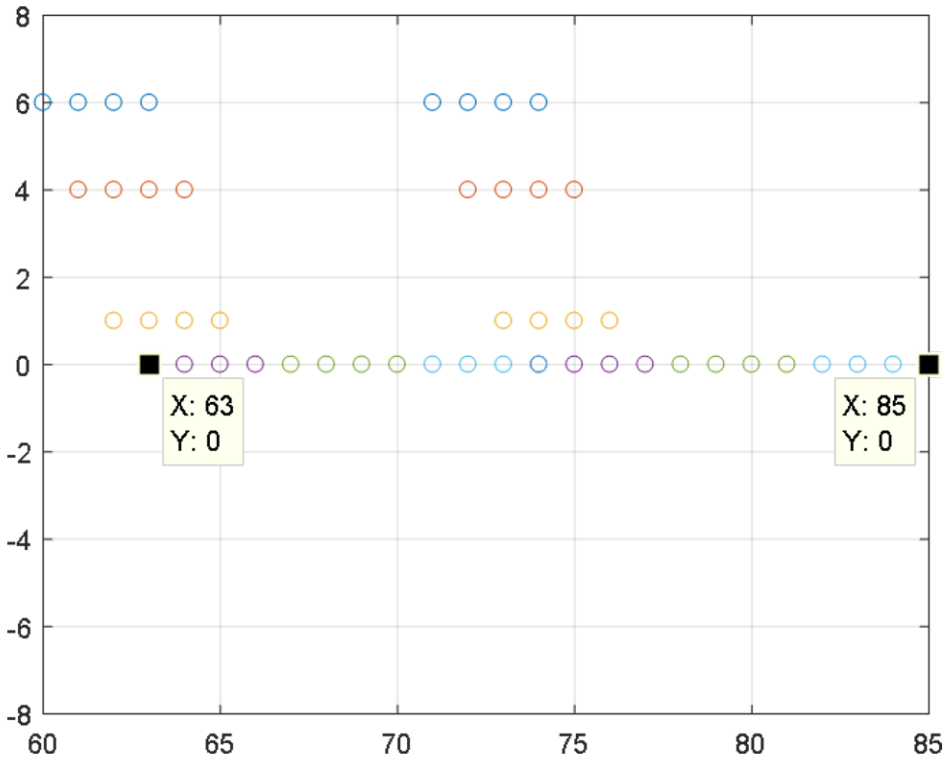

3.2 Chirp Configuration

Chirp configurations are different for MIMO and TXBF use cases.

3.2.1 Chirp Configuration for MIMO Radar

For the MIMO application, the chirp configuration in 表 2 is used.

表 2. Chirp Configuration - MIMO

PARAMETER	SRR	MRR
Idle time (µs)	5	4
ADC start time (µs)	6	5
Ramp end time (µs)	40	23
Number of ADC samples	256	256
Frequency slope (MHz/µs)	79	15
ADC sampling frequency (MSPS)	8	15
Number of chirps per frame per TX	128	128
Effective chirp time (µs)	34	17
Bandwidth (MHz)	2528	256
Frame length (ms)	69	4.4

With this chirp configuration the MIMO performance specified in 表 1 is achieved. The primary goal was to achieve a maximum distance of about 150 m and maximum velocity of +/- 130km/h. See Programming Chirp Parameters in TI Radar Devices for more details. As mentioned in the previous section, in MIMO mode, 6 antennae are used in azimuth and 3 in elevation. The 3 overlapped azimuth antennae cannot be used in MIMO. So, the total of chirps in a MIMO frame is 9 x "Number of chirps per frame per Tx." The Overlapped antennae are used for Vmax extension in TDM MIMO.

3.2.2 Chirp Configuration for TX Beamforming Radar

For the TX beamforming application, the chirp configuration in 表 3 is used.

表 **3. Chirp Configuration - TX Beamforming**

PARAMETER	SPECIFICATIONS
Idle time (µs)	4
ADC start time (µs)	5
Ramp end time (µs)	23
Number of ADC samples	256
Frequency slope (MHz/µs)	2.5
ADC sampling frequency (MSPS)	15
Number of chirps per frame	128
Effective chirp time (µs)	17
Bandwidth (MHz)	43
Frame length (ms)	3.5

With this chirp configuration the TXBF performance shown in 表 1 is achieved. The primary goal was to achieve a maximum distance of about 350 m and maximum velocity around +/-130 km/h. See Programming Chirp Parameters in TI Radar Devices for more details.

The amount of phase value to program to each TX channel is computed as a function of array factor and target angle. Assuming N TX channels, with TX1 as a reference, the distance between every other antenna and TX1 is the known distance when the antenna array is designed during board development. As shown in 图 9 for TI cascade EVM, the distance between any two adjacent TX channels is two times the wavelength.

图 **9. TX Array for Beamforming**

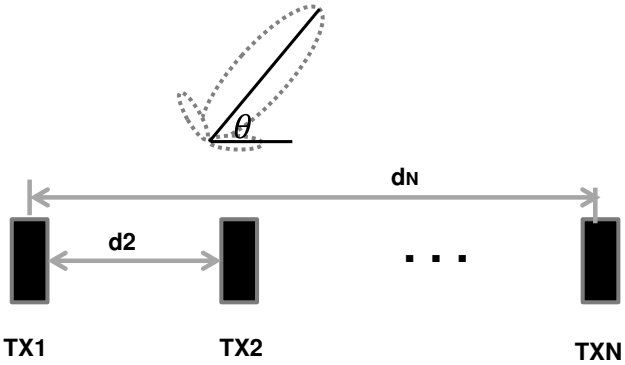

Given the notation in 图 9, the phase value for each TX channel is calculated as:

$$\overline{\varnothing} = [\varnothing_1, \varnothing_2, \varnothing_3 \ldots \varnothing_N] = \left[0 \;\; 2\pi\frac{d_2}{\lambda}\sin\theta \;\; 2\pi\frac{d_3}{\lambda}\sin\theta \;\; 2\pi\frac{d_N}{\lambda}\sin\theta\right] \quad (1)$$

The ideal phase value is further quantified by the allowed phase step size of 5.625 degree to calculate the integer value to be programed to the registers (TX calibration phase value will also be added as shown in the next section).

$$\overline{\varnothing_{int}} = \left\lfloor \frac{[\varnothing_1, \varnothing_2, \varnothing_3 \ldots \varnothing_N]}{5.625} \right\rfloor \quad (2)$$

As an example, for TI cascade EVM, 9 azimuth TX antennas can be used for beam steering, with [d2 = 2λ,d3 = 4λ,…,d9 = 16λ]. If the desired steering angle is 30 degrees, then the phase vector is as shown in degrees in 公式 3.

$$\overline{\varnothing} = \frac{[0 \;\; 4\pi \sin 30° \;\; 8\pi \sin 30° \;\; \ldots \;\; 32\pi \sin 30°]}{\pi} \times 180 \quad (3)$$

The TX beamforming application supports both chirp based beam steering and frame based beam steering. Advanced frame configuration is used for either case.

3.2.2.1 Chirp Based Beam Steering

In the subframe used for TX beamforming, the number of chirps used in this subframe is equal to the number of different desired steering angles. Each chirp configuration is associated with phase values for the TX array, calculated based on the corresponding desired steering angle. Within a burst, all chirp configurations are looped over till the end of the burst. 图 10 demonstrates the mechanism of chirp based beam steering.

图 10. Chirp Based Beam Steering

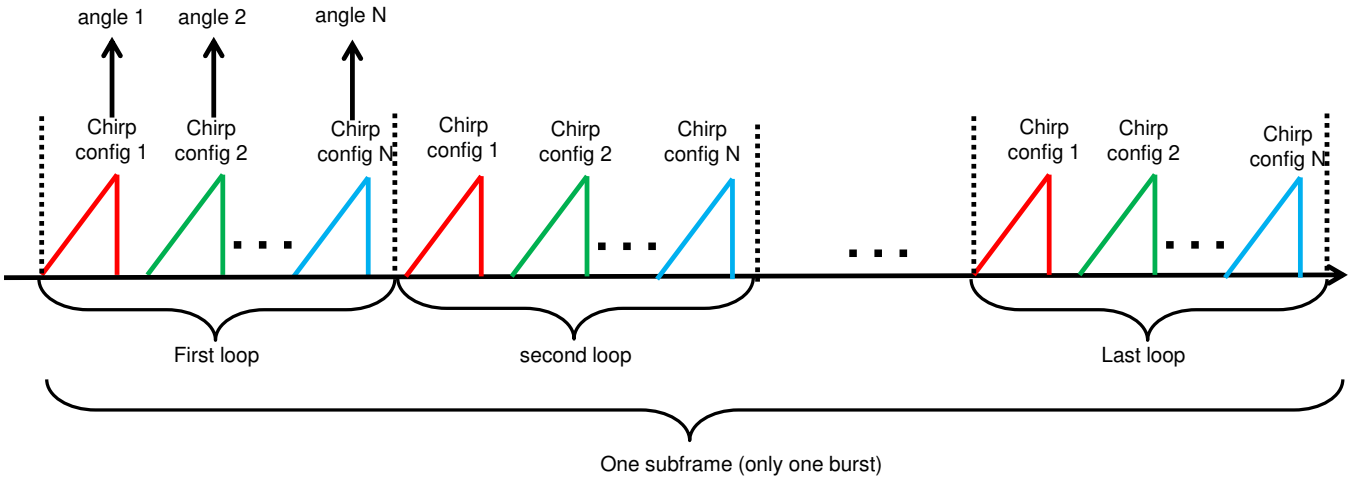

3.2.2.2 Frame Based Beam Steering

In the subframe used for TX beamforming, the number of burst within this subframe is equal to the number of different desired angles (same as number of chirp configurations). Each burst is associated with each chirp configuration, so a burst is equivalent to a frame within which each chirp has the same phase shifter value. 图 11 demonstrates the mechanism of frame based beam steering.

图 11. Frame Based Beam Steering

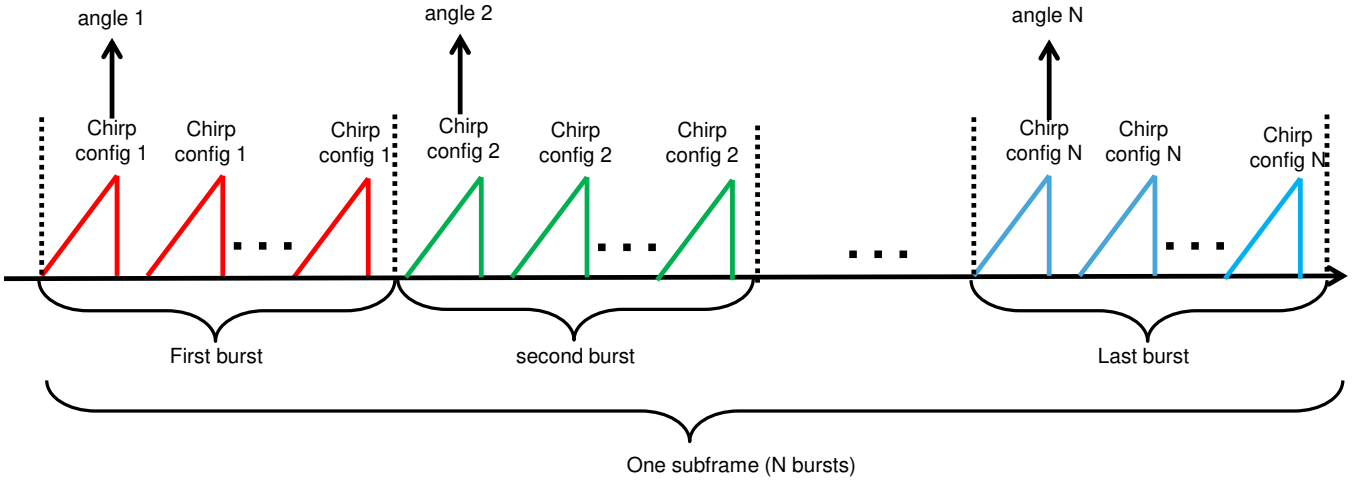

3.3 Antenna Calibration

The purpose of antenna calibration is to estimate the frequency, phase and amplitude mismatches across one master device and three slave devices. The mismatches can be caused by various reasons, such as path length mismatch, chip to chip variation, antenna coupling, and so on. The frequency mismatch is usually minimized by routing path length match during the board layout stage. The calibration method proposed by TI development kit is a one-time boresight calibration method. It is suggested to perform board specific calibration to achieve best angle performance.

3.3.1 How To Generate Phase/Gain Calibration Matrix

To generate a calibration matrix, it is suggested to put a corner reflector at distance of 5 m and beyond, with a typical corner reflector RCS of 1 m^2 to approximately 2 m^2, as shown in 图 12. The corner reflector should be aligned with the array center of board in both azimuth and elevation direction. A level sensor with laser pointer can be used for alignment.

图 12. Antenna Calibration Setup

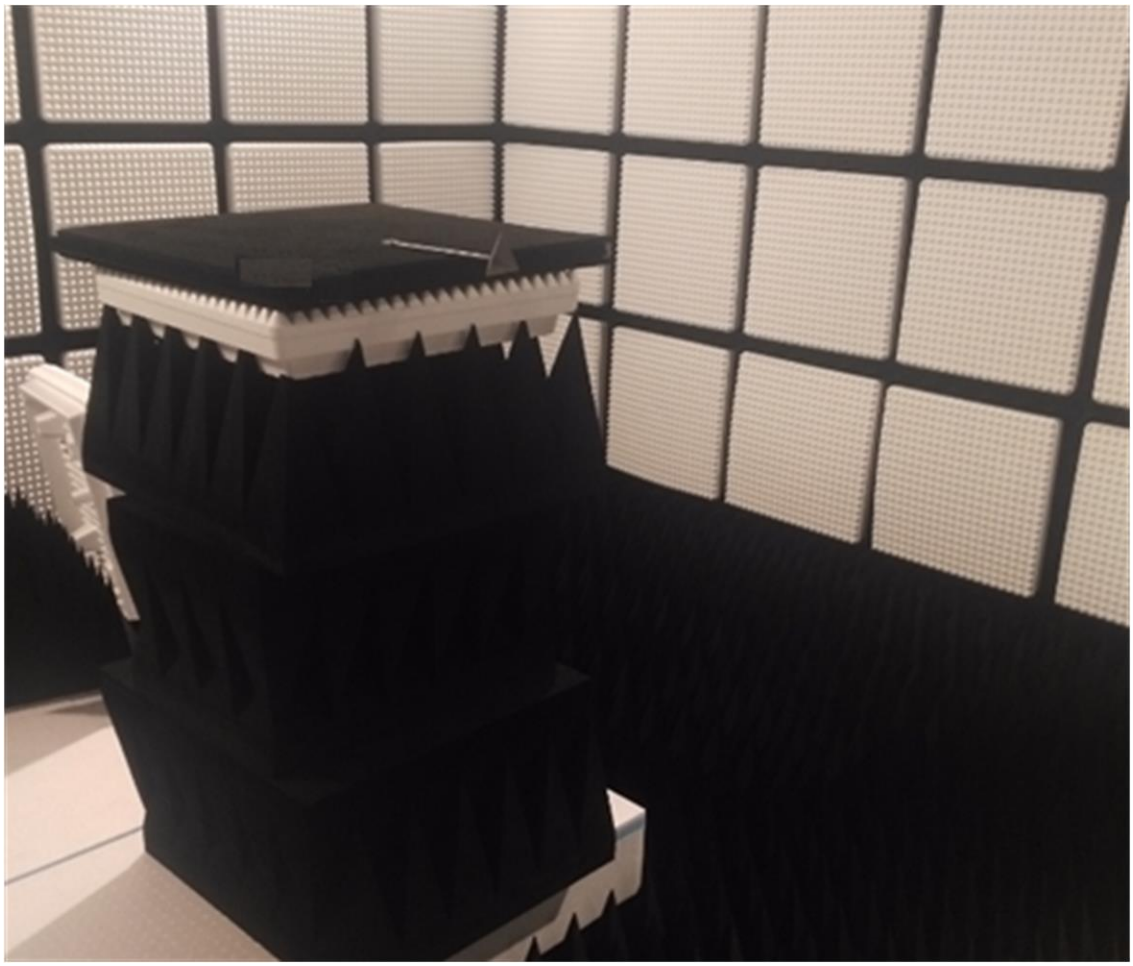

When the corner reflector is placed at the center position, a few frames of raw ADC data needs to be collected by using the example script provided in the mmWave Studio release. During the data collection, turn on 12 TX in a TDM MIMO mode and all 16 RX channels are on at the same time.

The calibration matrix generation follows the sequence described by 图 13. After the raw binary data is read and formatted so that data from 192 virtual channels are separated. Range FFT is performed on each channel and the peak corresponding to the corner reflector is identified as the local maximum within [D – 1, D + 1] meters, where D is the approximate target range provided by user. The FFT peak index from all 192 channels form a matrix size of 12 x 16, which will be used for frequency calibration step. The complex values at the peaks from all 192 channels form a complex calibration matrix of size 12 x 16, which will be used for phase and amplitude calibration. These two matrixes are saved to a matlab .mat file to be loaded when applying the calibration results to the ADC data.

图 13. Flow to Generate Phase and Gain Calibration Matrix

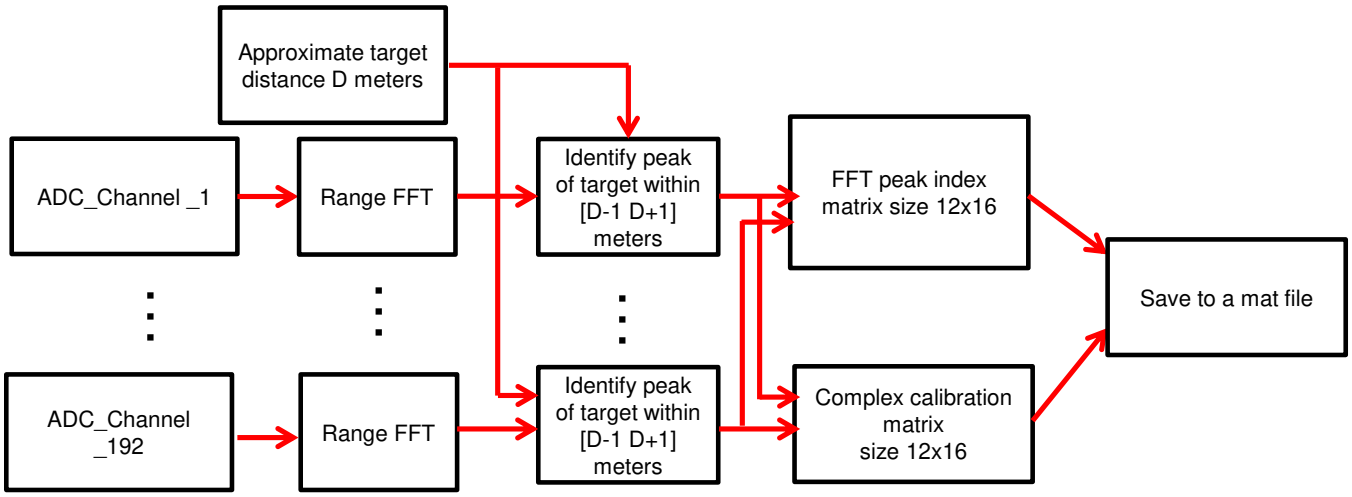

3.3.2 Applying Calibration For MIMO Operation

The saved calibration information is applied to the raw ADC data collected in MIMO mode in two steps on the flow shown on 图 14.

3.3.2.1 Frequency Calibration

The FFT index of TX1/RX1 channel is used as reference that is compared with all the other 191 channels. The FFT index difference and chirp parameters are used to compute the frequency calibration vector using 公式 4.

$$\vec{F} = 2\pi \times \Delta P \times \frac{\frac{f_s^{calib}}{f_s^{chirp}} \times \frac{f chirp}{f calib}}{\left(N \times I_{interp}\right)} \times \vec{n} \quad (4)$$

where

- ΔP is the FFT peak index difference for a virtual channel
- f_{chirp} is the FMCW chirp frequency slope
- f_{calib} is the FMCW chirp frequency slope used for calibration which can be different from f_{chirp}
- N is the number of ADC samples per chirp
- $\vec{n}$= [0 N-1] is the ADC sample index
- I_{interp} is the interpolation factor used for frequency calibration that is further explained in the next section
- $\vec{F}$is the computed frequency calibration vector
- exp(-j×$\vec{F}$) is multiplied with the raw ADC data for frequency calibration
- fs^{calib} is the FMCW chirp sampling rate used for calibration which can be different from the sampling rate fs^{chirp}

For each virtual channel, $\vec{F}$is calculated and applied to the corresponding ADC data

3.3.2.2 Phase and Amplitude Calibration

After frequency calibration, the phase and amplitude calibration value is calculated based on the complex value of the reference channel

$$C_{ph\_am} = \frac{C_{ref}}{C_{txi/rxj}}$$

where

- C_{ref} is the complex value of the reference channel
- $C_{txi/rxj}$ is the complex value of the other channels
- $C_{ph_am}$is the calculated phase and amplitude calibration value

C_{ph_am} is 1 for reference channel and different for every other channel

$C_{ph_am}$is multiplied with the output from the frequency calibration and the result is the final calibrated ADC data (5)

图 14. Flow to Apply Calibration Matrix to ADC Data

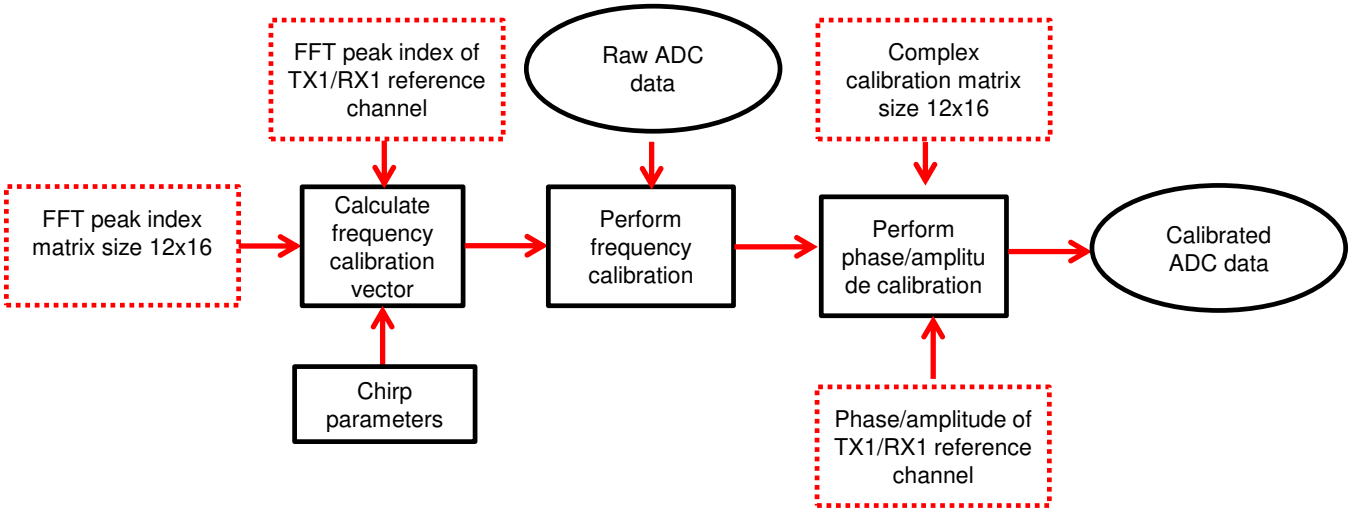

3.3.3 Applying Calibration For TX Beam-forming Operation

The saved calibration information is applied in TX beamforming operation as shown in 图 15. The phase value of the 12 × 16 complex value matrix obtained from section “How to generate calibration matrix” is averaged across the 16 RX channels to obtain a phase calibration vector for the 12 TX channels. According to the index of TX channel used in actual TX beamforming mode, the corresponding phase value within this 12 × 1 vector is used for the phase compensation. The compensation phase value together with the phase value calculated based on the desired steering angle is used to program the phase shift register value before starting beam steering process.

图 15. Calibration in TX Beamforming

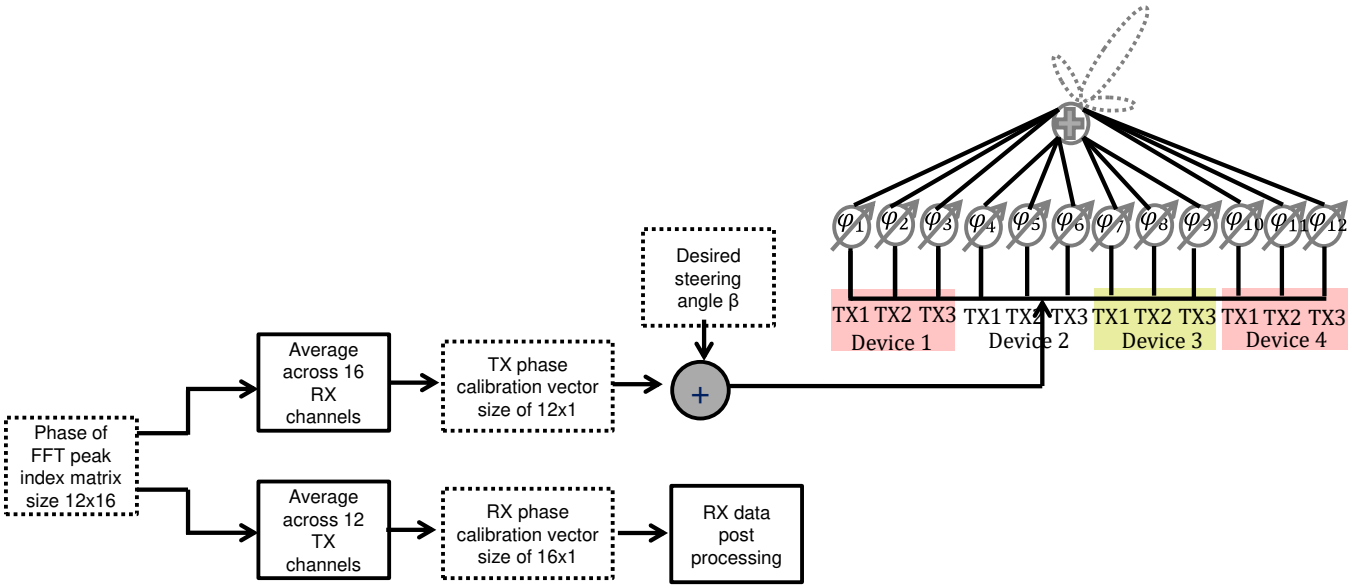

Similarly, the phase across the 12 TX channels is averaged to obtain a phase calibration vector for the 16 RX channels. This is phase only RX calibration assuming that there is no frequency mismatch across the 16 RX channels. The frequency mismatch across 16 RX channels can be captured by collecting calibration data by following these steps.

1. Put a corner reflector at a known distance, for example, approximately 6 m
2. Configure all TX channels to steer towards zero degrees
3. Check the FFT peak index of all 16 RX channels; the FFT peak index indicates the frequency mismatch, similar to the frequency mismatch described in 节 3.3.2.

The phase calibration value is applied during the RX data post processing stage. More details will be discussed in the signal processing section of TX beamforming.

3.4 Cascade Radar Signal Processing Chains

3.4.1 MIMO Signal Processing Chain

The raw signal collected in MIMO mode is processed in the flow shown in 图 16.

图 16. MIMO Signal Processing Chain

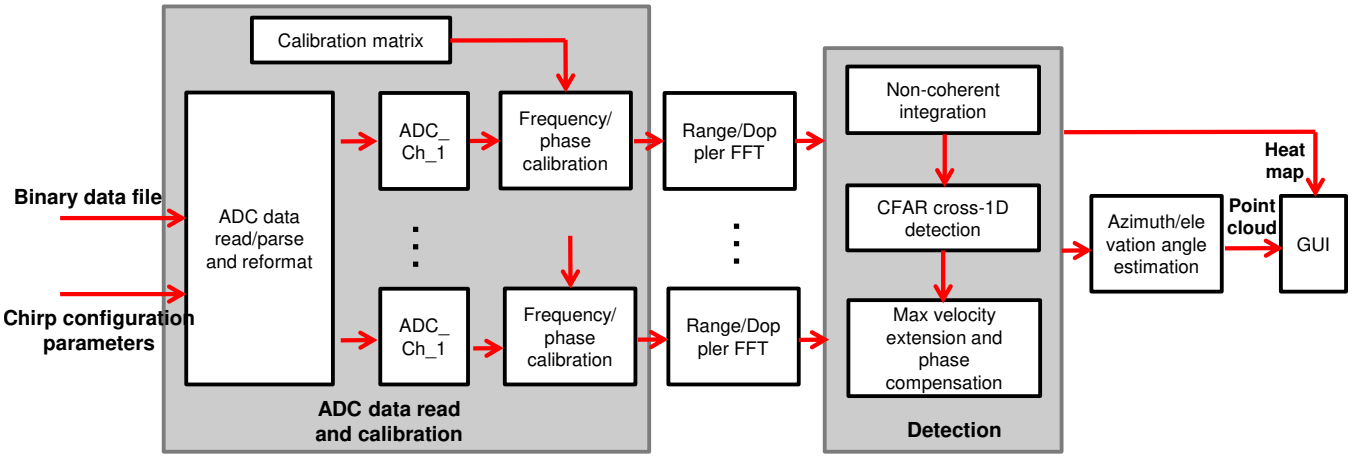

3.4.1.1 ADC Data Read and Calibration

After each data collection, a binary data file corresponding to each of the four cascaded devices is saved as well as the corresponding chirp configuration file. These two files are the inputs to the ADC data read and calibration module. The binary data file is read/parsed according to the chirp parameters based on the data format, samples per chirp, chirps per frame, number of TX/RX channels. Then the data is reformatted into a 4D matrix, with the dimension of samples per chirp, chirps per frame, number of RX channels, and number of TX channels. Each of the TX/RX channel is calibrated according the pre-calculated calibration matrix that can be obtained using the procedures as described in Section 3. (reference)

3.4.1.2 Range/Doppler FFT

For each TX/RX channel, range FFT is performed followed by Doppler FFT. The default windowing is a Hanning window. The FFT size is determined as the closest integer that is power of 2.

3.4.1.3 Detection

The output of range/Doppler FFT is sent to the detection module. The first step is non-coherent integration across all the virtual channels. The integration output goes through the CFAR detection step that does 1D range CFAR detection followed by 1D Doppler CFAR detection at the detected range bins. For each cross detected range/Doppler point, the maximum velocity extension algorithm is applied to correct any possible velocity ambiguity caused by TDM MIMO. The recovered velocity is used to correct the phase jump that is again caused by the TDM MIMO for each detected point.

3.4.1.4 Angle Estimation

For each detected point, angle estimation is performed based on the signal vector with corrected phase. If the configured array is azimuth direction only, only azimuth angle estimation is needed. If a 2D configured array is involved, both azimuth and elevation angle estimation is performed. Note that multiple angles will be detected in the azimuth direction, but only the maximum peak is selected in the elevation direction.

3.4.1.5 GUI

Point cloud and heat map can be sent to GUI for visualization.

3.4.2 TX Beamforming Signal Processing

This section provides an example signal processing chain in TX beamforming mode. Users might have their own preferred signal chain depending on the application. This example signal processing chain is used to generate an azimuth/range heat map by stitching multiple TX beamforming scans together.

图 17 shows the block diagram of the example signal processing chain in TX beamforming mode. The desired steering angles are defined as β1 β2 ... βn. For each angle βi, the phase shifter value is calculated based on the TX phase calibration vector and βi with given TX antenna positions (see 节 2.3.3). The received ADC data from each RX channel goes through range and Doppler FFT, and only zero Doppler bin is selected for range/azimuth heat map generation assuming it is a static test scene. For moving test scene, user needs to change accordingly. For each range bin at zero Doppler, after phase compensation using calibration vector, RX beamforming is performed to steer the RX beam towards the same βi where the TX channels are focusing on. As a result, one range line is generated for each angle βi. By stitching all the lines generated with different βi angles, a range/azimuth heat map is generated.

图 **17. TX Beamforming Signal Processing Chain**

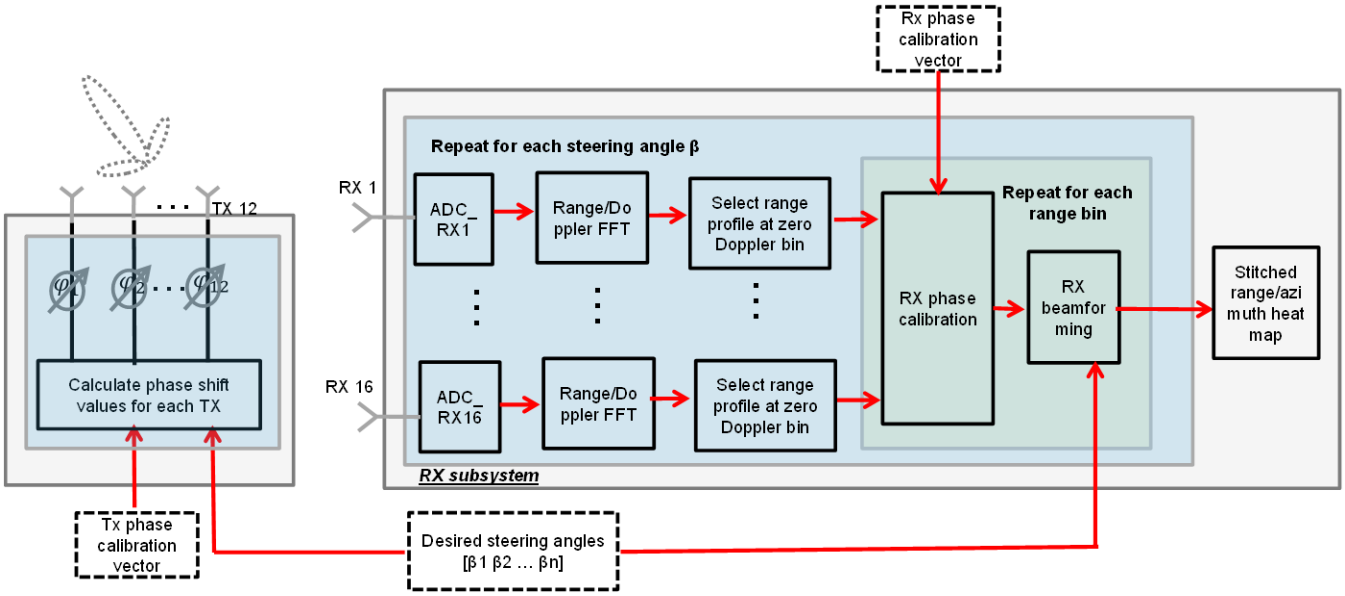

图 18 shows the example heat map results. Two corner reflectors are separated by around 1.8 degrees at 6 m within the anechoic chamber. The anechoic chamber size is around 6 m in width and 12 m in length. The radar is put around 4 m away from one side. The top left and top right plots are the heat map results (top-down view) running in MIMO mode and stitched TX beamforming mode. The TX beam is steering within [–60 60] with step size of 0.5 degree. The rectangular shape corresponding to the anechoic chamber wall, and the two bright spots in the middle are corresponding to the two corner reflectors. The bottom left and bottom right plots are the heat map results in a 3D view, with the height indicates the reflection intensity. The separation of the two peaks is more visible in the 3D view. It is worth to note that the grating lobes caused by the wide distance of adjacent TX channels are no longer observed because of the cancellation in the RX beamforming process.

图 **18. Heat Map – MIMO and Stitched TX Beamforming – Top Down View**

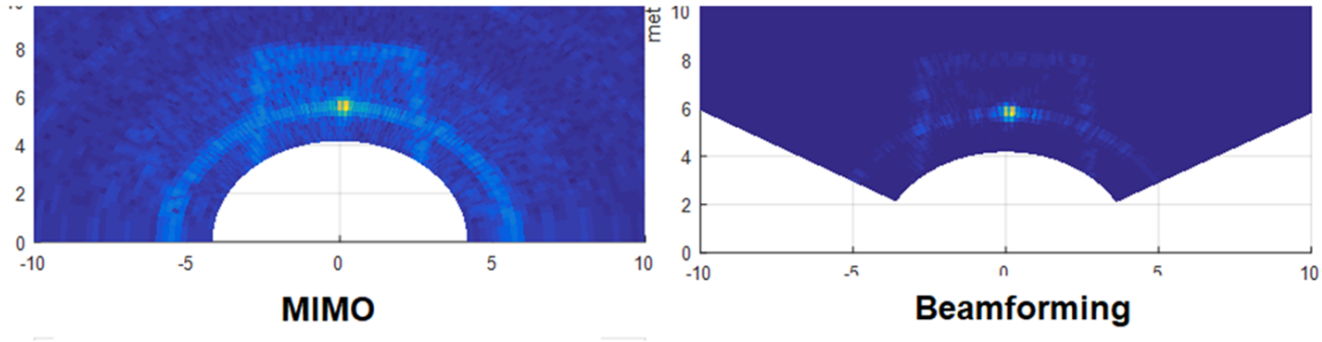

图 **19. Heat Map – MIMO and Stitched TX Beamforming – 3D View**

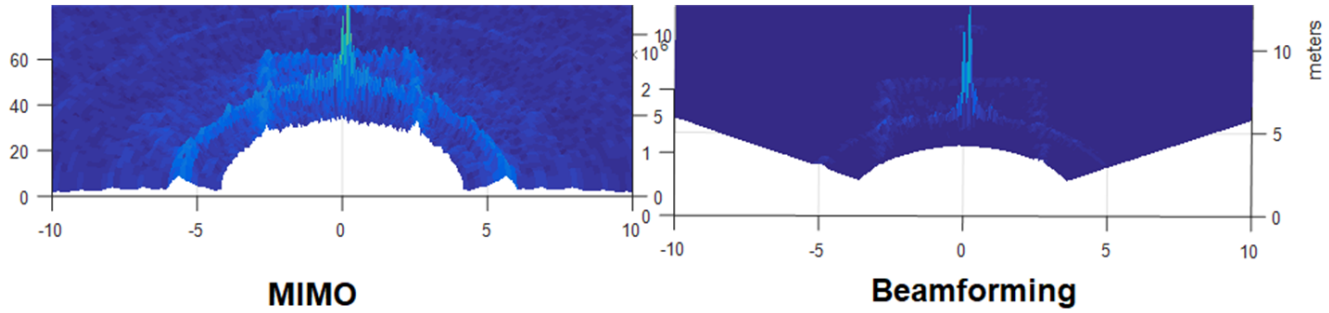

This experiment result proves that the receiver angle resolution in these two operation modes are equivalent since the effective aperture size is the same. Further, the signal SNR in the beamforming is much higher due to the coherent gain in TX beamforming mode. The SNR in MIMO mode can be improved by increasing the chirp integration time.

4 Hardware, Software, Testing Requirements, and Test Results

4.1 Required Hardware and Software

4.1.1 Hardware

The tests were performed using the older generation AWR1243P four-device Cascade Radar RF board from Texas Instruments together with TDA2 based capture System. With the newer generation of the sensor, AWR2243, the RF performance is improved as shown in the AWR2243 data sheet.

图 **20. Four-Device Cascade Radar RF Board with TDA2 Based Capture Board**

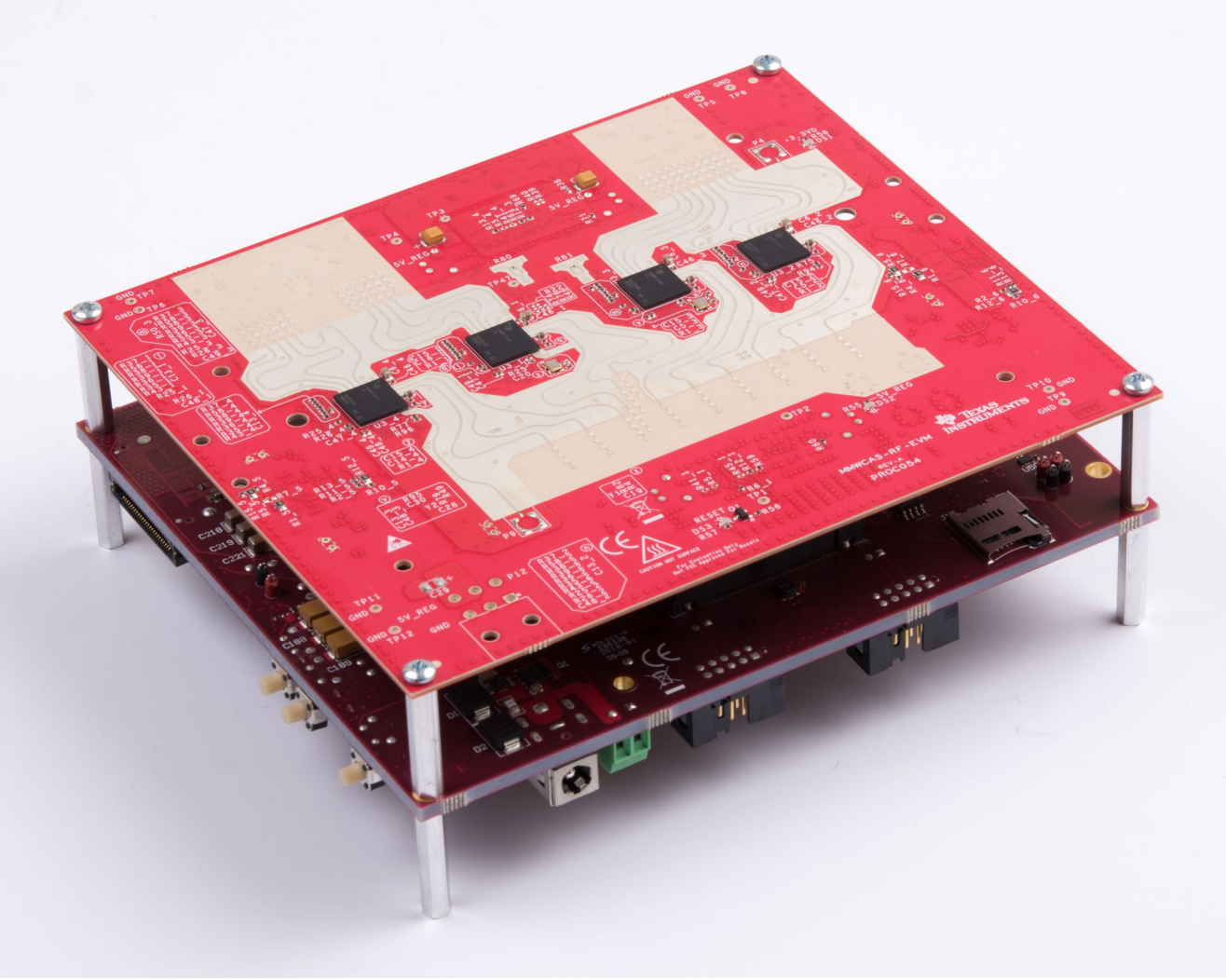

4.1.2 Software

The cascade board was configured using an updated version of the MMWAVE-STUDIO tools. Algorithms implemented in Matlab were used to post process the captured raw data.

4.2 Testing and Results

Multiple test scenarios were setup to explore the capabilities of the Cascade Radar RF design in both MIMO and TX beamforming operation.

All data presented here was collected with the Hardware mentioned above.

4.2.1 Test Scenarios

4.2.1.1 MIMO Test Scenarios

- In-lab Angular Resolution
- Side-by-side Car Detection Resolution
- Car, Pedestrian and Other Targets Close Range Separation
- Car Contour and Orientation
- Car Door Contour
- Bike Contour and Orientation
- Fence Contour Detection
- Curb Contour Detection

4.2.1.2 TX Beamforming Test Scenarios

- In-lab Beamforming Control Pattern
- Pedestrian Long-Range Detection
- Car Medium-Range detection
- Car Long-Range Detection

4.2.2 MIMO Test Results

4.2.2.1 In-lab Angular Resolution

A basic azimuth separation test was performed within an anechoic chamber radar test range. Two corner reflectors were placed with an angular separation of approximately 1.5 degrees at a distance of 8 m from the mmwave sensor.

In the current configuration, with 86 virtual array elements in the azimuth axis, and lambda/2 spacing of each element, a best-case 1.4 degree angular resolution is possible. This system measured a 1.5 degree separation, which is close to the expected value.

图 **21. Two Corner Reflectors Separated by 1.5 Degrees in Azimuth**

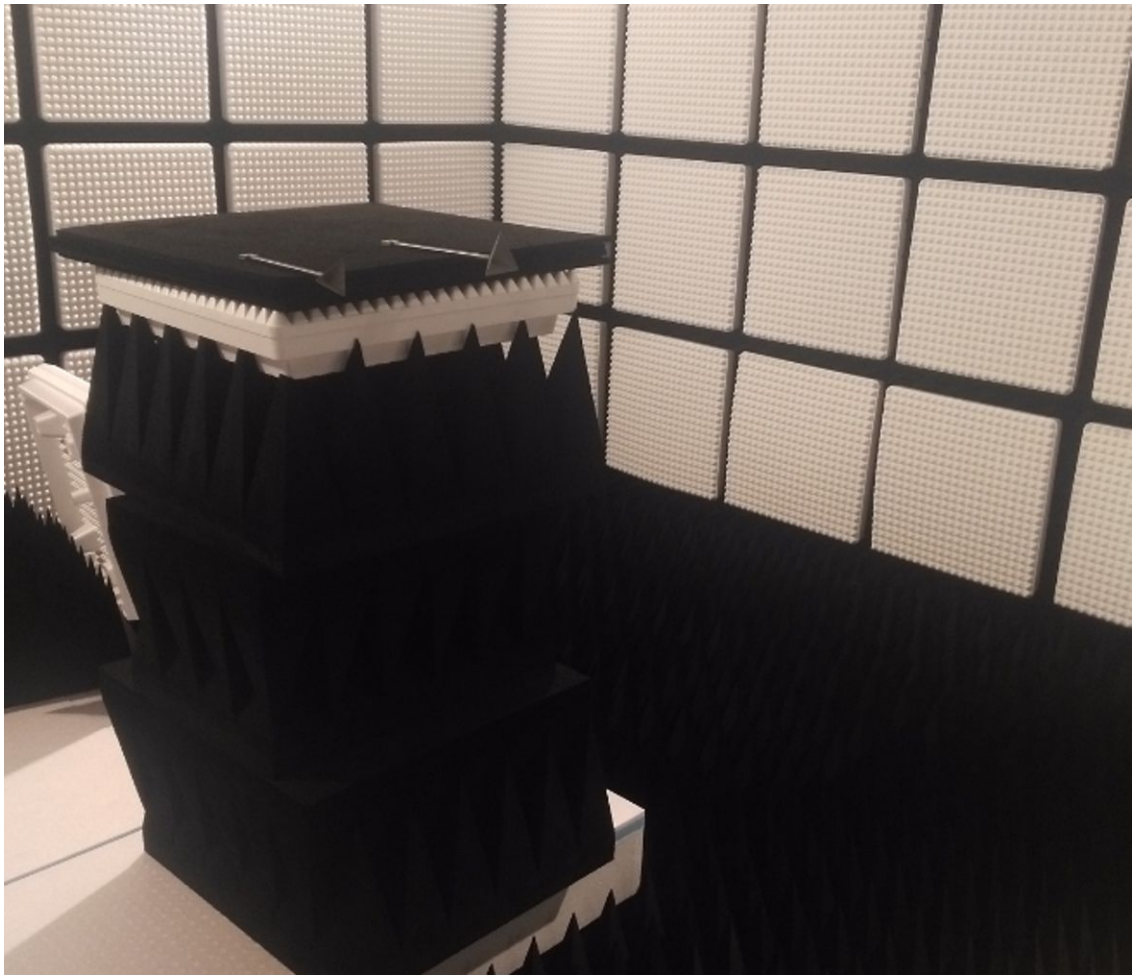

图 **22. Range-Doppler FFT Plots Showing Detected, Separated Peaks From Both Reflectors**

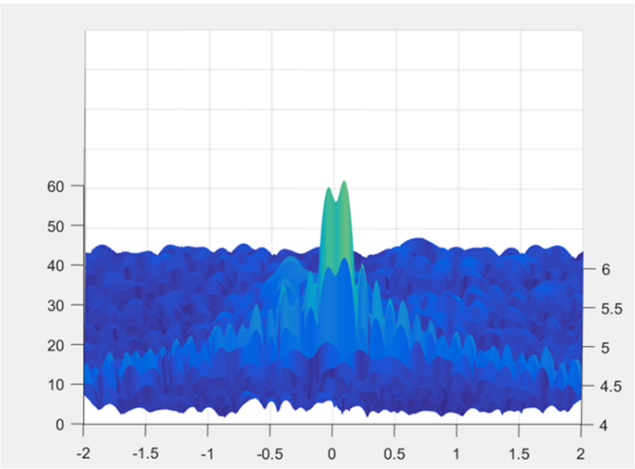

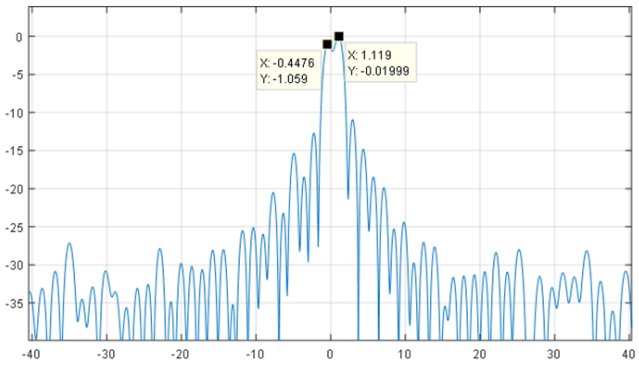

4.2.2.2 Car Angular Resolution Scenario

A test was performed with two cars located at 112 m range from the sensor at varying angular separations, again showing the angular resolution capabilities of the AWR2243 MIMO radar operation.

图 **23. Two-Car Angular Separation Test Setup**

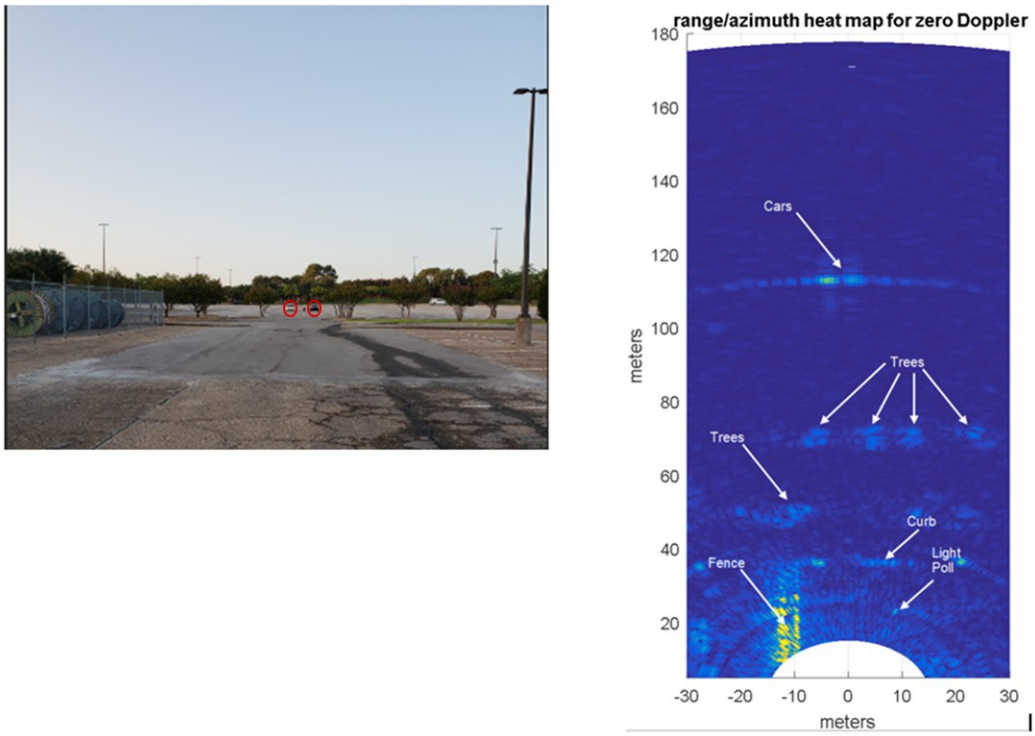

图 **24. Two-Car Angular Separation Test Results**

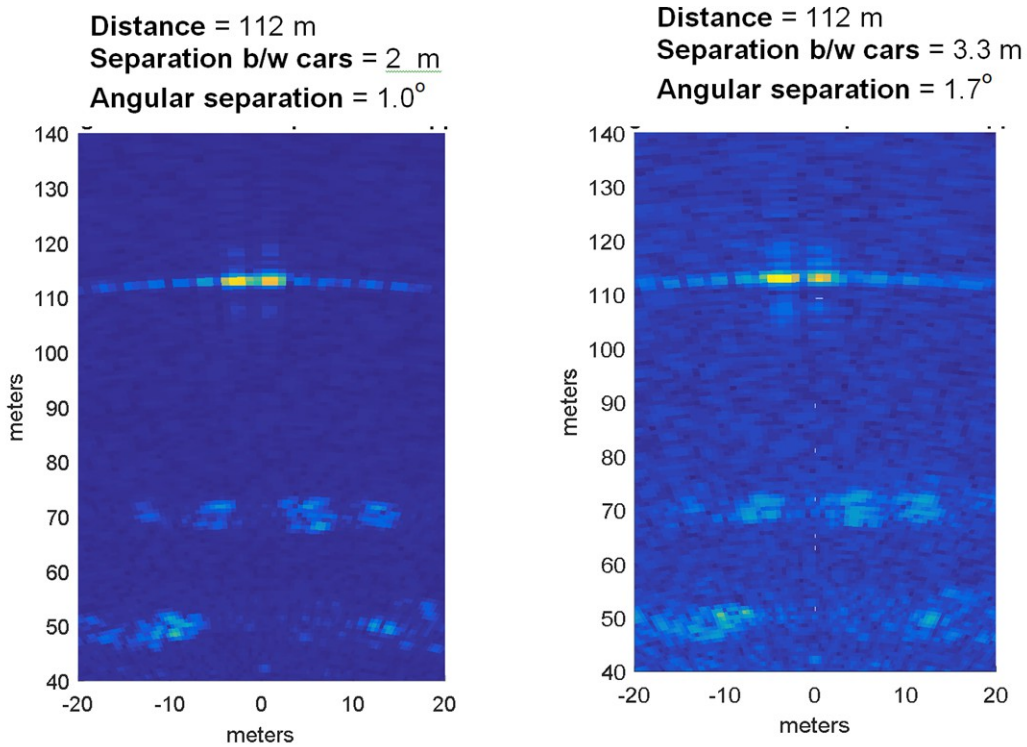

4.2.2.3 Car, Pedestrian, and Other Targets Close Range Separation

A test was performed showing the AWR2243 MIMO radar is able to separate a person and a bicycle at different lateral distances away from the car. This would be challenging in scenarios where a pedestrian (or another low RCS object) is occupying the same range-bin as a car (high-RCS object)

图 **25. Bicycle and Person 1.5 Meters Away From Vehicle**

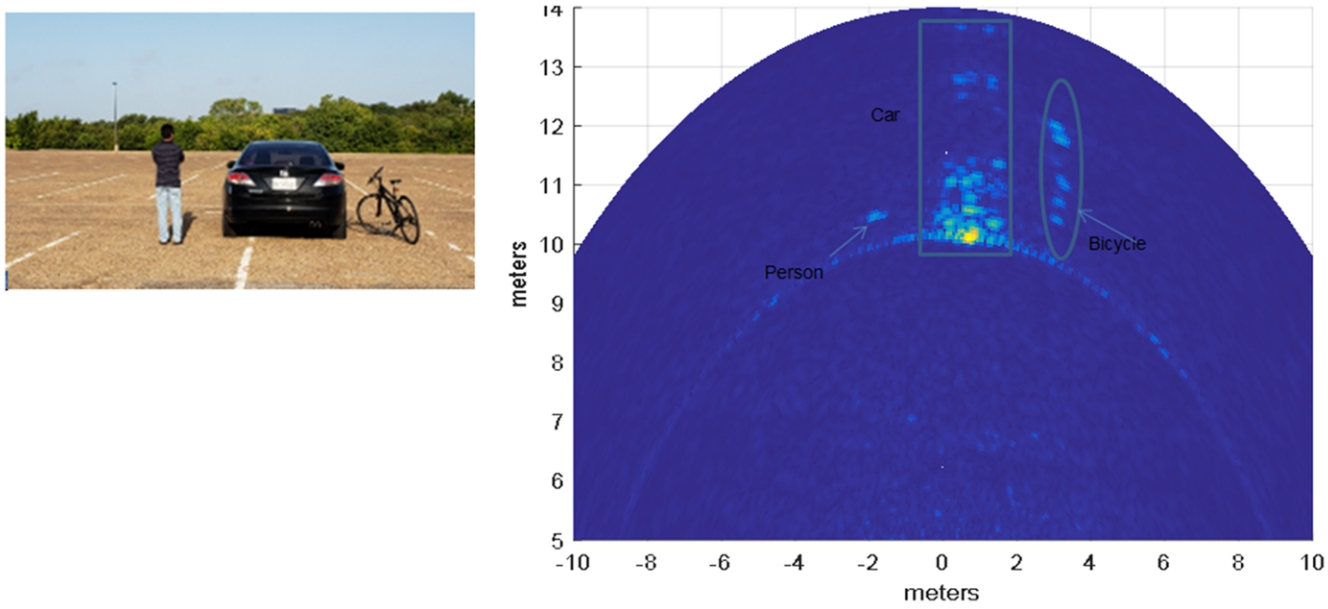

图 **26. Bicycle and Person 1.0 Meter (left) and 0.5 Meter (right) Away From Vehicle**

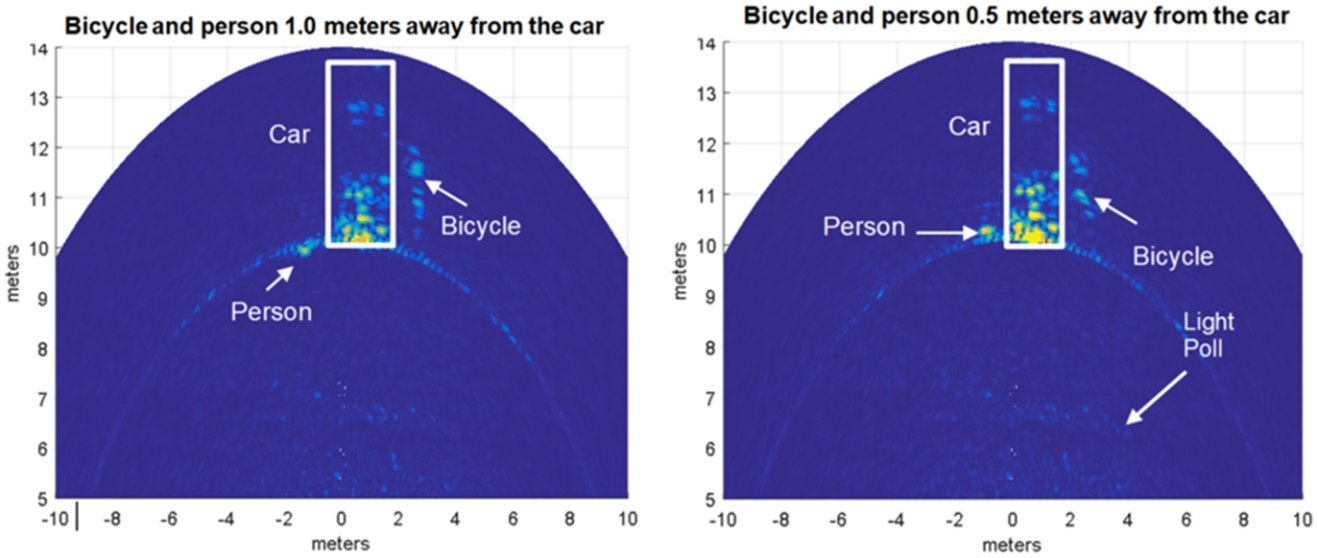

4.2.2.4 Car Contour and Orientation

A test was performed showing the AWR2243 MIMO radar detecting the contour and orientation of a car. The azimuth and range resolution allows for the detection of the contour of many vehicle surfaces.

图 27. Car at 0 Degrees (Top) Car with Open Door (Bottom) Orientation and Corresponding Azimuth Range Heatmapp

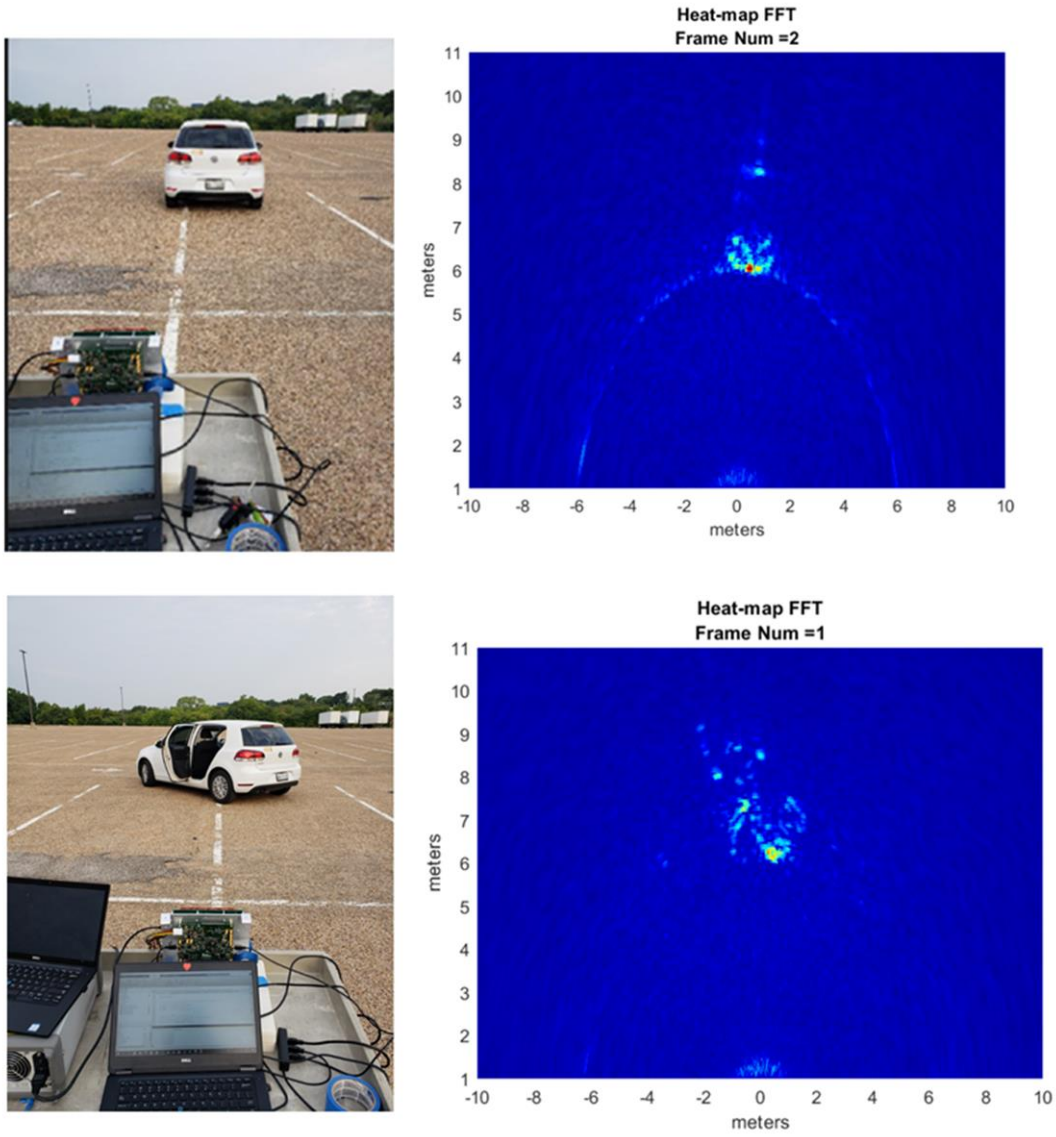

4.2.2.5 Curb Contour Detection

A test was performed showing the AWR2243 MIMO radar detecting the contour and orientation of multiple curbs in a parking lot setting. The azimuth and range resolution allows for the detection of the contour of these shorter driving obstacles.

图 28. Parking Lot Curb Scene (Top), and Resulting Azimuth Range Heatmap (Bottom)

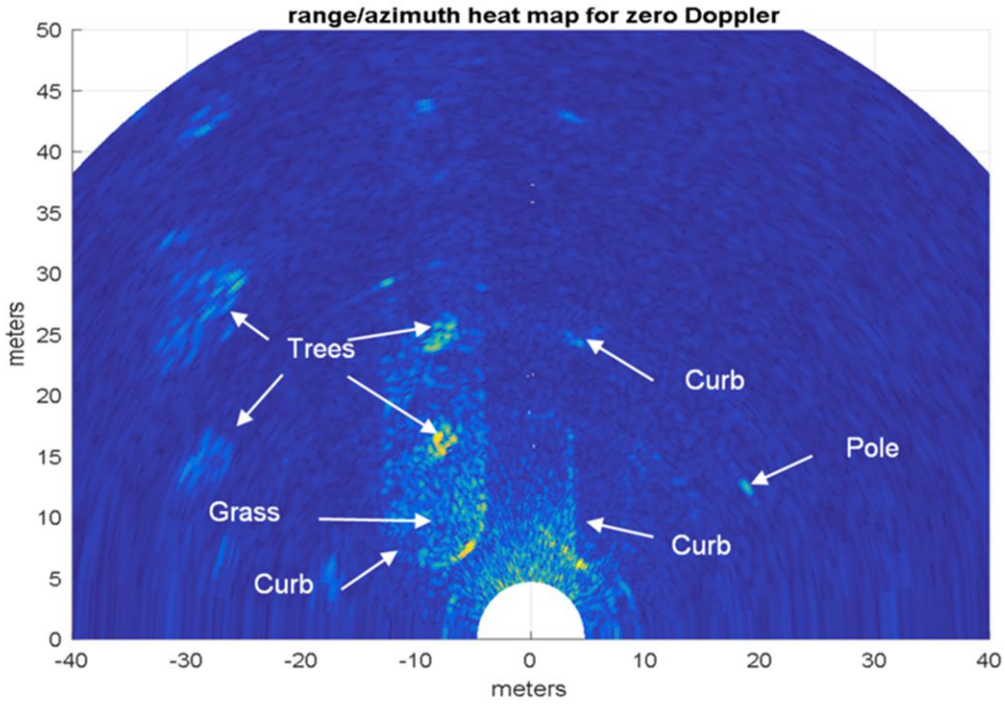

4.2.3 TX Beamforming Results

4.2.3.1 In-lab Beamforming Control Pattern

A basic beam steering test was performed within an anechoic chamber radar test range. A single corner reflector was placed approximately 8 m from the AWR2243 radar sensor. Beamsteering vectors were then programmed into the AWR2243 devices to achieve a 15 degree beam rotation. The resulting target return versus angle graph was then compared against the simulated 15-degree beam rotation pattern.

Close alignment between the simulated and measured system was observed.

图 **29. Simulated (Top) and Measured (Bottom) 15 Degree Beam Steering Test**

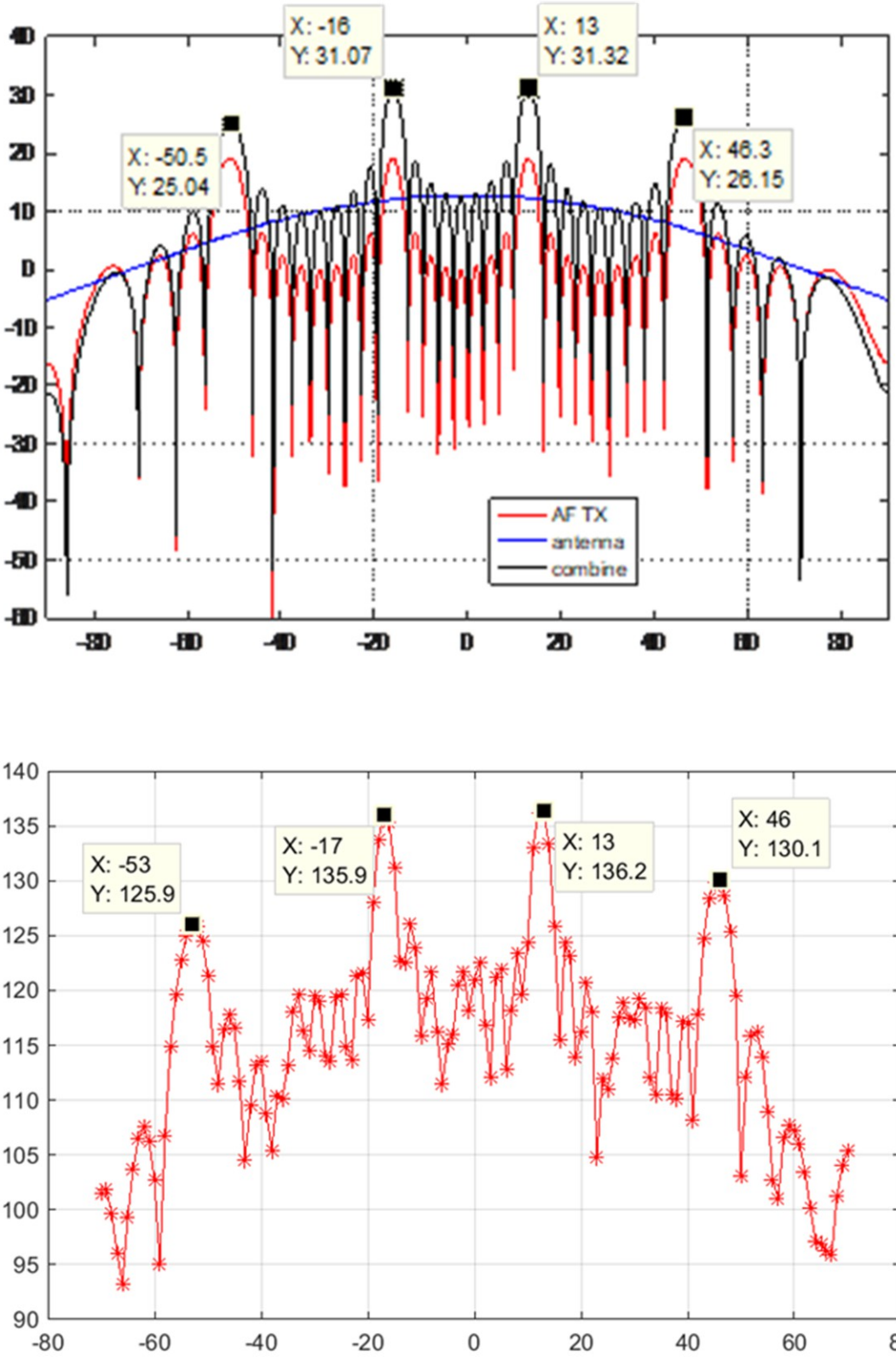

4.2.3.2 Pedestrian Long-Range Detection

In this test a pedestrian jogging from 30 m to 140 m. The AWR2243 Cascade RF board is running in 9-TX beamforming mode.

The range profile shows the pedestrian at 120 m with 20-dB SNR. The Doppler-Range plot is shown to the right. Slight Doppler displacement can be seen corresponding to the pedestrian velocity.

图 30. Range Profile (top left), and Doppler-Range Plot of a Pedestrian Jogging Away From Radar at 120 Meters Range

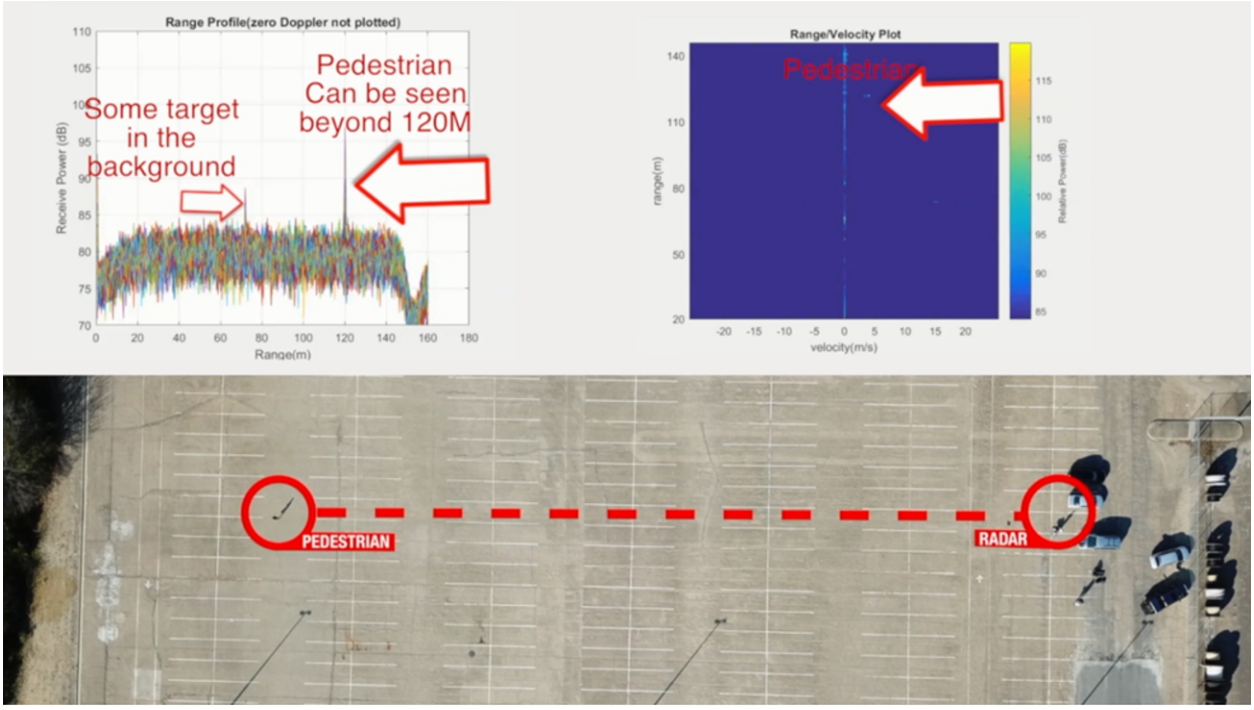

4.2.3.3 Car Long-Range Detection

Similar to the pedestrian long range detection test, this test observes a car at 350-m range. The AWR2243 Cascade RF board is running in 9-TX beamforming mode.

The range profile shows the vehicle at 350 m with 14-dB SNR.

图 **31. Range Profile (left), and Doppler-Range Plot of a Vehicle 350 Meters Range**

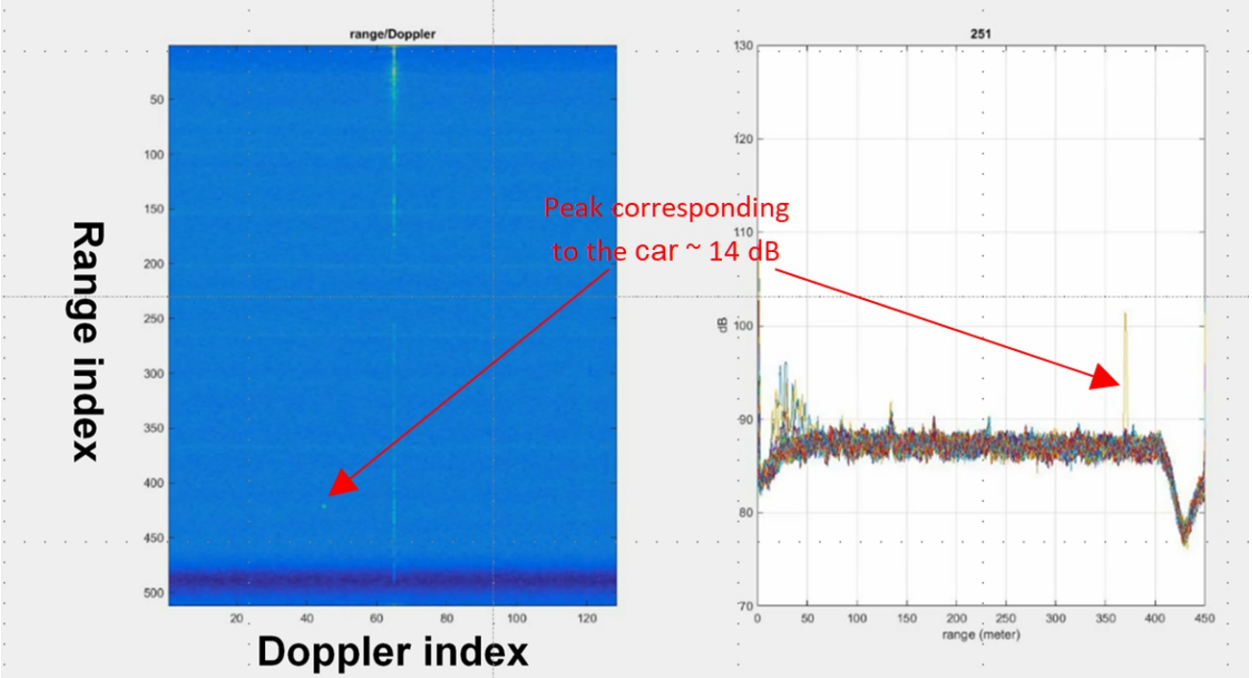

5 Design Files

5.1 Schematics

To download the schematics, see the design files at TIDEP-01012.

5.2 Bill of Materials

To download the bill of materials (BOM), see the design files at TIDEP-01012.

5.3 Altium Project

To download the Altium Designer® project files, see the design files at TIDEP-01012.

5.4 Gerber Files

To download the Gerber files, see the design files at TIDEP-01012.

5.5 Assembly Drawings

To download the assembly drawings, see the design files at TIDEP-01012.

6 Software Files

The cascade board was configured using an updated version of the MMWAVE-STUDIO tools.

7 Related Documentation

1. Texas Instruments, *Programming Chirp Parameters in TI Radar Devices Application Report*
2. Texas Instruments, *AWR2243 76-GHz to 81-GHz High-Performance Automotive MMIC*
3. Texas Instruments, *AWR2243 Cascade Application Report*
4. Texas Instruments, *MMWAVE-STUDIO*

7.1 商标

E2E is a trademark of Texas Instruments.
Altium Designer is a registered trademark of Altium LLC or its affiliated companies.
Arm, Cortex are registered trademarks of Arm Limited.

7.2 Third-Party Products Disclaimer

TI'S PUBLICATION OF INFORMATION REGARDING THIRD-PARTY PRODUCTS OR SERVICES DOES NOT CONSTITUTE AN ENDORSEMENT REGARDING THE SUITABILITY OF SUCH PRODUCTS OR SERVICES OR A WARRANTY, REPRESENTATION OR ENDORSEMENT OF SUCH PRODUCTS OR SERVICES, EITHER ALONE OR IN COMBINATION WITH ANY TI PRODUCT OR SERVICE.

修订历史记录

注：之前版本的页码可能与当前版本有所不同。

Changes from Original (June 2019) to A Revision **Page**

- 已更改 通篇将 *AWR1243* 更改为 *AWR2243* 1
- 已添加 添加了*此设计指南中提供的数据是从使用 AWR1243P 器件的 MMWCAS-RF-EVM 版本 C 中获得的。然而，最新的 MMWCAS-RF-EVM 版本 D 使用了第二代 AWR2243 器件。此 AWR2243 解决方案应该作为未来设计的参考。* 1
- 已添加 添加了 MMWCAS-RF-EVM 工具文件夹 1
- 已更改 将*检测物体* 更改为*显示物体检测* 1
- 已添加 添加了（在方位平面中） 1
- 已更改 *AWR1243* to *AWR2243* in the GHZ LO Distribution Block Diagram 8
- 已更改 *16 RX* to *8 RX* 11
- 已删除 *For the MIMO application, to achieve the system performance specified above, the chirp configuration in 表 2 is used.*to *For the MIMO application, the chirp configuration in 表 2 is used.* 11
- 已更改 *(kSPS)* to *(MSPS)* 11
- 已添加 *per TX* 11
- 已更改 cross-reference from *Table 2* to *Table 1* 12
- 已更改 *maximum unambiguous velocity of 133 km/h* to *maximum velocity of +/- 130km/h* 12
- 已删除 The choice of the chirp periodicity is a trade-off between range resolution and maximum velocity. The velocity resolution is defined by the number of chirps per frame. 12
- 已添加 As mentioned in the previous section, in MIMO mode, 6 antennae are used in azimuth and 3 in elevation. The 3 overlapped azimuth antennae can't be used in MIMO. So, the total of chirps in a MIMO frame is 9 x "Number of chirps per frame per Tx." The Overlapped antennae are used for Vmax extension in TDM MIMO. 12
- 已删除 *...to achieve the system performance specified above,* 12
- 已更改 *256* to *128* 12
- 已更改 *256* to *43* 12
- 已更改 *4.4* to *3.5* 12
- 已更改 *133* with *+/-130* 12
- 已删除 ...the number of chirps used in this subframe is equal to the number of different desired steering angles. Each chirp configuration is associated with phase values for the TX array, calculated based on the corresponding desired steering angle... 13
- 已更改 *After each data collection, a binary data file and the corresponding chirp configuration parameters are saved.* to *After each data collection, a binary data file corresponding to each of the four cascaded devices is saved as well as the corresponding chirp configuration file.* 19
- 已删除 *The details of maximum velocity extension and phase compensation will be discussed in a separate section.* 19
- 已更改 *grading* to *grating* 20
- 已更改 *...using the AWR2243 four-device* to *...using the older generations AWR1243P four-device* 22
- 已添加 With the newer generation of the sensor, AWR2243, the RF performance is improved as shown in the AWR2243 data sheet 22
- 已删除 Side-by-side Car Detection Resolution – MUSIC Algorithm 23
- 已删除 Manhole Contour Detection, Height Measurement, Single-Device vs. Cascade Devices 23
- 已更改 *Two corner reflectors were placed approximately 8 m from the AWR2243 radar sensor. 1.5 degrees of azimuth separation was applied to the reflectors and the resulting azimuth resolution was measured.* to *Two corner reflectors were placed with an angular separation of approximately 1.5 degrees at a distance of 8 m from the mmwave sensor* 23
- 已更改 *which is in close alignment to the expected.* to *which is close to the expected value.* 23
- 已更改 *Car at 0 Degrees (Top), 90 Degrees (Middle) and 135 Degrees (Bottom) Orientation and Corresponding Azimuth Range Heatmap* to *Car at 0 Degrees (Top) Car with Open Door (Bottom) Orientation and Corresponding Azimuth Range Heatmap*Replaced image with new image 27

重要声明和免责声明

TI“按原样”提供技术和可靠性数据（包括数据表）、设计资源（包括参考设计）、应用或其他设计建议、网络工具、安全信息和其他资源，不保证没有瑕疵且不做出任何明示或暗示的担保，包括但不限于对适销性、某特定用途方面的适用性或不侵犯任何第三方知识产权的暗示担保。

这些资源可供使用 TI 产品进行设计的熟练开发人员使用。您将自行承担以下全部责任：(1) 针对您的应用选择合适的 TI 产品，(2) 设计、验证并测试您的应用，(3) 确保您的应用满足相应标准以及任何其他功能安全、信息安全、监管或其他要求。

这些资源如有变更，恕不另行通知。TI 授权您仅可将这些资源用于研发本资源所述的 TI 产品的应用。严禁对这些资源进行其他复制或展示。您无权使用任何其他 TI 知识产权或任何第三方知识产权。您应全额赔偿因在这些资源的使用中对 TI 及其代表造成的任何索赔、损害、成本、损失和债务，TI 对此概不负责。

TI 提供的产品受 TI 的销售条款或 ti.com 上其他适用条款/TI 产品随附的其他适用条款的约束。TI 提供这些资源并不会扩展或以其他方式更改 TI 针对 TI 产品发布的适用的担保或担保免责声明。

TI 反对并拒绝您可能提出的任何其他或不同的条款。

邮寄地址：Texas Instruments, Post Office Box 655303, Dallas, Texas 75265